A Phylogenetic Approach to Bryozoan Morphology

Jeroen Pieter Boeve

Master of Science thesis

Centre for Ecological and Evolutionary Synthesis
Department of Biosciences
Faculty of Mathematics and Natural Sciences

University of Oslo

2016

2016

A Phylogenetic Approach to Bryozoan Morphology

Author: Jeroen Pieter Boeve

II

A Phylogenetic Approach to Bryozoan Morphology

IV

Abstract

Bryozoa is a large phylum of colonial invertebrates with a rich fossil history. By far the largest order, the Cheilostomata, is particularly interesting for the study of macroevolutionary questions as many morphological traits that clearly reflect ecological function and life history are frequently preserved in the fossil record. However, the systematics of this order is still largely based on morphological traits. Key taxonomic revisions have been suggested based on recent molecular studies on multiple taxonomic levels within cheilostomes, but there are a vast number of relationships to be resolved and evolutionary questions still to be answered. Therefore, through the addition of previously unsequenced cheilostome taxa to existing sequence information on bryozoan taxa, this study aims to establish the most extensive, highly resolved molecular phylogenetic hypothesis of bryozoans to date. Finding *Steginoporella* as a robustly placed sister group to Electridae, lends credit to the notion that brooding has evolved independently multiple times within cheilostomes. Frontal shield evolution has been hypothesised to be important drivers of the rapid cheilostome diversification during the mid-Cretaceous, but no statistical test has been applied to verify this idea. I hence used this newly established phylogeny of cheilostomes to study two grades of frontal shields, Anasca and Ascophora, using a phylogenetic comparative model that simultaneously estimates diversification rates and trait evolution I find that ascophorans have an overall higher diversification rate, either because of higher speciation rates or because of lower extinction rates, compared to anascans.

Acknowledgements

I wish to sincerely thank Paul Taylor, for his enthusiastic introduction to the world of Bryozoa when he came to the university here in Oslo. Also, his taxonomic knowledge and comments have been most helpful during the writing of this thesis. Andrea Waeschenbach, for spending one week in the laboratory with me and fellow bryophiles; to teach us the secrets to molecular studies of Bryozoa! The help you provided then, and ever since, has been much appreciated and critical to the success of this thesis. Emanuela Di Martino, for being there to answer any questions, and all the lovely Bryo-lunches you shared with the group.

The three wonderful people mentioned above, and many more who I met at the Larwood Symposium in Scotland in 2015. You all made a difference in my view on science as people from different fields came together to share their fascination with bryozoans.

I'd like to thank Abigail Smith, Seabourne Rust, Antoniette Rosso, Joanne Porter and Matt Dick for providing samples. Dennis Gordon for sending many samples and helping me with the taxonomy in general.

Nanna Winger Steen, Emelita Rivera Nerli and Cecilie Mathiesen for doing a wonderful job with the labs, and the lovely Friday morning labmeetings.

Thanks to all the friends I made during my stay here at the university. without you, learning wouldn't have been this fun. Also to the people who make lesesal 3320, well… "lesesal 3320!". A truly unique and crazy place to spend two years. Emily Enevoldsen and Mali Ramsfjell, we've gone through this bryozoan adventure together, and it has truly been a blast! Thank you.

A big thank you to the people who are closest to me. My family, whom I love dearly. And Tynke, who supported me through my years as a master's student. You've been far away in distance, but never closer to my heart.

At the point of writing, I have yet to realise my time as a master student is soon over. I'm certain that future me, wherever he may be, will look back at the past two years and remember nothing but an amazing, inspiring, and educational time. Two years which have been made possible by three of the most amazing supervisors.

Russell Orr, you've been a wonderful teacher. Most of my time as a master's student has been in the lab under your supervision. You have a way of explaining things and engaging people with close-to-perfection analogies, which I really appreciate.

Kjetil Lysne Voje you are an extremely inspiring person. Your jolly personality and motivational words have made my day, many times!

Lee Hsiang Liow, it is in your nature to question,.. everything! And it is clear that you've amassed huge amounts of knowledge because of it. Your curious nature is inspiring, and I'm grateful for being allowed to tap into that wisdom. You've been my main supervisor during my years as a master student, and I could not have asked for a better candidate.

I'm truly and sincerely grateful that I have been given the opportunity to work with all three of you. Given the chance, I'd chose the same project, with the same people, in a heartbeat!

Jeroen Boeve,

Blindern, September 1st, 2016

Table of Contents

1   Introduction

Phylogenetic hypotheses are immensely important in the field of biology. A good understanding of the phylogenetic history of a taxonomic group enables us to compare different models of their evolutionary history and explore the underlying mechanisms of macroevolution. One phylum with a great potential for studying the patterns and processes of macroevolution is Bryozoa. Bryozoans are a large group of about six thousand described extant species (Bock and Gordon 2013) many of which with the ability to bio-mineralize. Consequently, bryozoans have a relatively rich fossil record where specimens are frequently very well-preserved. Not only do their fossils tell a story of species occurrences, many of them also retain important morphological traits despite taphonomic processes, making them exceptionally suited for studying trait evolution. Phylogenies of bryozoans have traditionally been based solely on morphological traits. This is problematic due to the high levels of convergent evolution and phenotypic plasticity within the group (Waeschenbach et al. 2012, Taylor et al. 2015) such that many traditionally recognized clades have collapsed, based on molecular work (Waeschenbach et al. 2012). To increase our understanding of phylogenetic relationships among bryozoans, the phylum desperately needs more extensive phylogenetic hypotheses, encompassing a larger amount of data, in terms of both taxa and sequences. The work done by Waeschenbach et al. (2012) has been a leap forward in our understanding of bryozoans. However, only 1-2 % of all bryozoans are currently part of a phylogenetic hypothesis based on molecular data. With this in mind, I present my main aim of this study, which is to sequence more taxa in order to infer phylogenetic relationships among a greater representation of bryozoan taxa so as to increase our understanding of past changes in bryozoan morphology.

Bryozoans are colonial: they may be found on shells, stone, and even sand grains (Taylor 2005). The main bulk of bryozoan species are marine, while some groups live in freshwater habitats, such as the Phylactolaemata (Porter et al. 2002). Most colonies start out as a sexually-produced larva settling down on a substrate, after which metamorphosis occurs and genetically identical zooids are laid down by budding. Some new colonies may form asexually from fragments of previously established colonies, due to their clonal nature (Jackson 1985). While individual zooids in a given colony are genetically identical, they may take on different morphologies called polymorphs (McKinney and Jackson 1991, Lidgard et

al. 2012). Examples of polymorphs include feeding zooids also known as autozooids, avicularia and ovicells (Gordon et al. 2009).

There are three classes within the Bryozoa phylum: Phylactolaemata, Stenolaemata, and Gymnolaemata (fig. 1) (Fuchs et al. 2009, Hausdorf et al. 2010, Waeschenbach et al. 2012). The Cheilostomata order is one of two orders within the gymnolaemates. It has by far the highest abundance today, both in terms of species richness and ecological abundance. The order represents approximately 80 percent of all bryozoan species. They have a wide range of morphological traits such as ovicells, avicularia, different larval types and frontal shields. The latter is one of the key subjects of this study and will be explained in more detail later. All aforementioned traits are thought to have been repeatedly evolved among cheilostomes. The vast range of easily observable morphologies compared to the other bryozoan clades, together with a good fossil record, makes cheilostomes a suitable candidate for the in-depth study of evolutionary questions. For this reason I focus on the cheilostome bryozoans and aim to increase taxonomic sampling of this group. Among the samples available to me, there are multiple taxa representing families which have yet to be placed in a phylogenetic hypothesis.
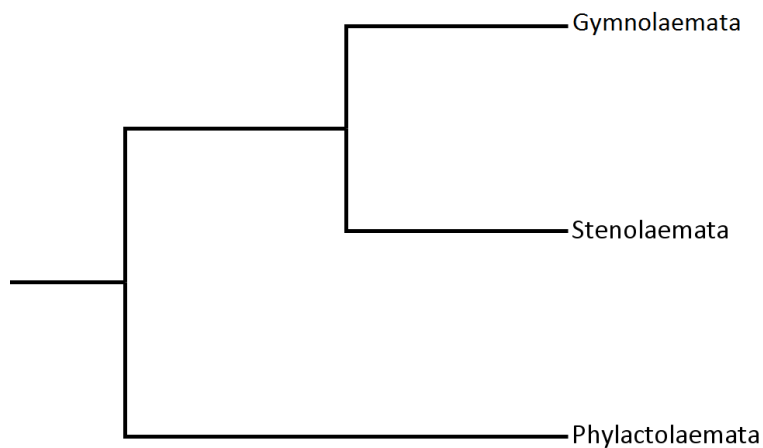
Figure 1: Relationship among the three bryozoan classes redrawn from Taylor and Waeschenbach (2015).

The cheilostome order has traditionally been divided into two suborders based on a single morphological character. The Anasca have their frontal membrane overlying the calcified frontal shield, unlike the Ascophora, which have their calcified frontal shield over the frontal membrane. These groupings are non-monophyletic, and ascophoran organisation of the frontal wall is now thought to have arisen multiple times (Knight et al. 2011). Frontal shield

2

evolution has also been though to influence diversification rates and consequently species richness among bryozoans with anascan and ascophoran "states", as these traits may influence colonial level and species level survival. This brings me to the second aim of this thesis which is to look at the effect of anascans and ascophorans frontal shields on rates of speciation and extinction. To this end, I perform a Binary State Speciation and Extinction (BiSSE) (Maddison et al. 2007) analysis to infer the effect of frontal shield type on speciation, extinction, and transition rates among cheilostome bryozoans. Using ancestral state reconstruction based on an extension of the BiSSE model, I will also infer when in geological time specific frontal wall types, including malacostegan, lepraliamorphan, and umbomulomorphan types evolved.

2   Materials and methods

The main aim of this project is to increase molecular sampling of bryozoans, by sequencing previously unsequenced taxa. I will first introduce the species samples and explain the protocols I used starting from a given sample to aligning the sequences I obtained from the samples. The resulting alignments ware then used to infer a phylogenetic hypothesis, which was in turn calibrated using fossil occurrences and used in further analyses of traits.

2.1   Sampling

The samples were collected in the period between 2007 and 2011 and have all been stored in >90% ethanol (Table 1). Morphological vouchers have been collected and scanning electron microscopy images taken for all the samples collected by Andrea Waeschenbach (Appendix 4 figures 1 through 17).

Table 1: Overview of samples. First column are species names. "?" are unconfirmed species descriptions. Second column are sample identification codes from A. Waeschenbach. Column 4: depths in meters where applicable. Country codes: NZ=New Zealand, UK=United Kingdom, NO=Norway. MD= missing data.

Species	Code	Location	Depth	Date of collection	Collector
Adeonellopsis sp(?)	AW301	-47.86 166.87, NZ	157m	30.01.2008	Abigail Smith
Aimulosia marsupium	AW725	Barrett's Reef, 5-11m, Wellington Harbour entrance, NZ	MD	25.01.2008	M. Carter
Akatopora circumsaepta	AW527	PU5; -46.10; 166.10, NZ	87m	17.01.2009	Abigail Smith
Arachnopusia unicornis	AW293	-47.91; 166.74, NZ	148m	02.02.2008	Abigail Smith
Beania magellanica	AW403	SN14; -47.32 167.49, NZ	107m	31.01.2008	Abigail Smith
Calwellia gracilis	AW632	NZ	MD	MD	Dennis Gordon
Cellaria sp.	AW532	PU1; -46.02 166.35, NZ	180m	17.01.2009	Abigail Smith
Crassimarginatella sp.	AW519	PU5; -46.10; 166.10, NZ	87m	17.01.2009	Abigail Smith
Crepidacantha zelanica	AW664	SN11, NZ	MD	MD	Abigail Smith & Joanne Porter
Cupuladria sp.	AW817	MD	MD	MD	Simon Coppard
Dimetopia cornuta	AW631	NZ	MD	MD	Dennis Gordon
Emma rotunda	AW633	NZ	MD	MD	Dennis Gordon
Euthyroides yellyae	AW533	PU5; -46.10 166.10, NZ	87m	17.01.2009	Abigail Smith
Figularia mernae	AW440a	SN4; -48.07; 166.67, NZ	143m	30.01.2008	Abigail Smith
Figularia sp.	AW596	OS20; -47.28 167.67, NZ	100m	26.01.2010	Abigail Smith
Galeopsis sp.	AW580	OS14; -46.93 168.16, NZ	39m	25.01.2010	Abigail Smith

Gephyrotes nitidopunctata	AW187	Vatlestraumen South, NO	MD	18.11.2008	A. Waeschenbach
Hippomenella sp	AW275	Otago Shelf; 45° 49.3'S, 170° 53.0'E, NZ	83m	22.11.2007	Abigail Smith
Margaretta barbata	AW514	PU5; -46.10; 166.10, NZ	87m	17.01.2009	Abigail Smith
Micropora sp.	AW592	OS20; -47.28 167.67, NZ	100m	26.01.2010	Abigail Smith
Odontionella cyclops	AW279	-46.70; 167.97, NZ	54m	03.02.2008	Abigail Smith
Opaeophora lepida	AW733	Barrett's Reef, 5-11m, Wellington Harbour entrance, NZ	MD	25.01.2008	M. Carter
Osthimosia socialis	AW377	SN16; -47.26 167.66, NZ	88m	31.01.2008	Abigail Smith
Otionella sp.	AW607	OS31; -47.26 167.41, NZ	40m	28.01.2010	Abigail Smith
Phaeostachys sp.	AW162	Church Island, Menai Strait, UK	MD	01.10.2008	A. Waeschenbach
Rhynchozoon sp.	AW675	Greta Point, Wellington, NZ	MD	11.01.2008	Abigail Smith & Joanne Porter
Steginoporella sp.	AW730	Barrett's Reef, 5-11m, Wellington Harbour entrance, NZ	MD	25.01.2008	M. Carter
Synnotum aegyptiacum	AW442	SN8; -47.51; 167.33, NZ	152m	31.01.2008	Abigail Smith

2.2 DNA extraction and PCR

From the larger sized samples I extracted a fragment a few mm^2 to one cm^2 in size for DNA extraction from larger colonies in which this is possible. I carefully did this under a stereoscope and attempted to obtain a fragment from the tip or growing part of the colony to avoid fouled bits, done to reduce molecular contamination (Waeschenbach et al. 2012). Before extraction, the sample was left at room temperature for five to ten minutes, allowing ethanol to evaporate. Other samples were scraped off a rock or similar substrate, in which case the ethanol was washed off with Phosphate-buffered saline (PBS) before DNA extraction. This was done by spinning the sample at low centrifugal force (<6 rcf), removing the supernatant (i.e. the ethanol) and then adding roughly one ml of PBS buffer. This step was repeated twice. I performed DNA extraction with the DNeasy Blood & Tissue Kit from Qiagen. I followed the protocol in accordance with the manufacturers' instructions with one modification. I used pestles to homogenize the sample and break the calcareous hard parts to ensure that all the soft tissue properly lysates. DNA quantity was estimated utilizing a NanoDrop 1000 Spectrophotometer (Thermofisher).

The choice of target loci was based on availability of sequence data. Because of different mutation rates and degrees of constriction some gene regions may be better suited for different taxonomic levels than others when doing molecular research (Simon et al. 1994). For example, the ribosomal subunits are highly conserved in both nuclear and mitochondrial DNA, because they are immensely important for basic cellular machinery to function (see (Hillis and Dixon 1991). Because of this they are considered to give a good phylogenetic signal when analyzing deeper phylogenetic relationships. Cytochrome c oxidase subunit 1 (cox1) and cytochrome b (cytb) are considered to be good markers when looking at lower taxonomic levels. By using multiple gene regions that evolve at different rates and concatenating them into a single, larger, dataset, there is a higher chance of obtaining a more resolved tree at different taxonomical levels. Therefore, I targeted the following loci using Polymerase chain reaction (PCR): Small nuclear ribosomal subunit (18S/ssrDNA), large mitochondrial ribosomal subunit (16S/rrnL), small mitochondrial ribosomal subunit (12S/rrnS), cytochrome c oxidase subunit 1 (cox1), cytochrome c oxidase subunit 3 (cox3), and cytochrome b (cytb), following Waeschenbach et al. (2012)

To obtain the gene sequences, I used published primers in addition to designing new primers, based on the cheilostome sequences used in Waeschenbach et al. (2012) (Table 2). The sequences were aligned as described in the following paragraph. A primer search was conducted using PrimaClade, an online application to search through many sequences for conserved regions suitable as primer sites (Gadberry et al. 2005). The annealing temperatures for the new primers were calculated online using OligoCalc version 3.26 (Gadberry et al. 2005). Gradient PCR runs were performed, to look for temperature optima for the primer combinations with and without 2.5 % DMSO (a salt solution used for making DNA strands more accessible to primers through the decreased chance of secondary structures of DNA forming). For PCR I used DreamTaq DNA polymerase (Thermofisher scientific), in addition to Phusion high-fidelity DNA polymerase (Thermofisher scientific). The reagent volumes for each reaction followed the manufacturers' recommendation. 3-5 µl template was used. 1 µl of each forward and reverse primer was added for non-degenerate primers, while degenerate primers were added in 2 µl volumes each, at a concentration of 10 mM. All reactions were run with 25 µl total volume. See table 2 for an overview over primers used and Appendix 2 Table A2.1 for PCR cycling profiles. To investigate the lengths and quality of the PCR products, I performed 1% agarose gel electrophoreses.

6

Purification was done using the Wizard SV Gel and PCR Clean-Up System from Promega, I followed the instructions as established in the protocol. 30 µl of nuclease water was used for elution, and DNA quantity was checked with NanoDrop. Sanger sequencing was performed by GATC Biotech. I used BioEdit version 7.2.5 (Hall 2004) to check quality of the resulting sequence chromatogram files. BLAST (Basic local alignment search tool) searches were performed with blastn to ensure bryozoan sequences had been obtained (Altschul et al. 1990).

Table 2: Primers used in this study. Column 2 directions: F=Forward and R=Reverse

Primer name	F/R	Sequence 5'->3'	Reference
Bryozoa_16SF	F	TSKWCCYTGTGTATSATGG	Waeschenbach et al. (2012)
Bryozoa_16SR	R	ARTCCAACATCGAGGT	Waeschenbach et al. (2012)
Bryozoa_12SF	F	TGCCAGCANHMGCGG	Waeschenbach et al. (2012)
Bryozoa_12SR	R	YTACTDTGTTACGACTTWTC	Waeschenbach et al. (2012)
Cheilo_12SF_seq	F	AAAGAGCTTGGCGGT	Waeschenbach et al. (2012)
Cheilo_12SR_seq	R	GACGGGCGATTTGT	Waeschenbach et al. (2012)
Cheilo12S627_F	F	ACAAATCGCCCGTCRWTC	This study
Cheilo12s257_R	R	CCGCCAAGCTYTTTAGGY	This study
cox1F_prifi	F	TTGRTTYTTTGGWCAYCCHGAAG	Waeschenbach et al. (2012)
cox1R_prifi	R	TCHGARTAHCGNCGNGGTATHCC	Waeschenbach et al. (2012)
cox1R_prifi_M13F(-20)	F	GTAAAACGACGGCCAGTCHGAR TAHCGNCGNGGTATHCCc	Waeschenbach et al. (2012)
F2bryCOI	F	CCTGGAAGTTTAATAGGAAATGAYCA	Knight et al. (2011)
R2bryCOI	R	CTCCTCCAGCAGGGTCRAA TGRTGACGAGAYGTNAYHCG	Knight et al. (2011)
Bryozoa_cox3F	F		Waeschenbach et al. (2012)
Bryozoa_cox3R_M13F(-20)	R	GTAAAACGACGGCCAGACHACR TCWACRAARTGTCAC	Waeschenbach et al. (2012)
Bryozoa_cytbF_B	F	AGGDCAAATRTCWTWYTGRGC	Waeschenbach et al. (2012)
Bryozoa_cytbR	R	GGNAGAAARTAYCAYYCWGG	Waeschenbach et al. (2012)
18e	F	CTGGTTGATCCTGCCAGT	Hillis and Dixon (1991)
Gymno300R	R	CCTAATAAGTGCGCCCTT	Waeschenbach et al. (2012)
Gymno300F	F	AAGGGCGCACTTATTAGG	Waeschenbach et al. (2012)
18p	R	TAATGATCCTTCCGCAGGTTCAC	Halanych et al. (1998)
Gymno1200R	R	GGGCATCACWGACCTG	Waeschenbach et al. (2012)
Cheilo18S156_F	F	GYAACTCCGGYGCTAATACATGC	This study
Cheilo18s1660_R	R	GCTGATGACTCGCVAGTACA	This study

2.3   Alignment and phylogenetic inference

I aligned sequences obtained from the National Center for Biotechnology Information (NCBI) (see Benson et al. (2013)) along with sequences from Enevoldsen (2016) using mesquite software version 3.04 (Maddison 2015). To code nucleotide sequences into amino acid sequences, I used blastx with the option to align against invertebrate mitochondrial genome sequences (see Gish and States (1993)). A complete overview over all used sequences may be found in appendix table 1. Final alignment was performed in MAFFT (Multiple Alignment using Fast Fourier Transform) version 7 (Katoh and Standley 2013). Nucleotide alignments were run with the automatic option, while the amino acid alignments were run with the E-INS-i Iterative refinement method (Altschul 1998). The resulting alignments were visually inspected using mesquite. I made single gene alignments for all 6 gene regions. To determine poorly aligned or phylogenetically uninformative positions, I used Gblocks version 0.91b (Castresana 2000). Parameters were set to be least stringent, to counter the exclusion of shorter motifs. To find the best fitting evolutionary models for the nucleotide datasets I used jModelTest2 (Darriba et al. 2012). I used Prottest 3.4.2 (Darriba et al. 2011) to find the optimal model for the amino acid datasets. All nucleotide based datasets supported a General Time Reversible model with invariable sites and variation among sites (GTR+i+g) while the protein datasets supported MtArt as the best evolutionary model also with invariable sites and variation among sites, based on Akaike information criterion (AIC). I inferred the single-gene alignments using Randomized Axelerated Maximum Likelihood (RAxML) with100 topology inferences and 100 bootstrap runs (Appendix 2 figure A2.1 through A2.6) with evolutionary substitution models set as defined by the model tests. Taxa with an unstable phylogenetic affinity were identified and removed using RogueNaRok, I considered values over 0.5 to be detrimental. To concatenate all 6 datasets, Mesquite was used. I checked whether the concatenated dataset suffered from any leftover rogues by utilising RogueNaRok as pervious. I removed long branches to counter long branch attraction (LBA)(Bergsten 2005). To increase phylogenetic support, taxa with a high proportion of missing data were removed. Datasets with 10, 20, 30, 40, and 50 percent position requirement were run in RAxML using the same parameters as previous. The final dataset was run in RAxML with 100 topology searches and 500 bootstrap searches. Bayesian inference was performed in MrBayes version 3.2.2 (Ronquist and Huelsenbeck 2003). 60 million generations were run with a sampling rate of once every 1000th generation. 4.2 million generations were discarded as burn-in, after evaluation in Tracer v1.6 (Rambaut et al. 2014). As MrBayes lacks MtArt, rtREV (the second

best evolutionary model identified from Prottest) was used for both Bayesian (MrBayes) and ML (RAxML) phylogenetic inference. To check for congruence between the Bayesian and ML trees I used the Icong index (de Vienne et al. 2007).

2.4 Morphological analyses

To understand if and how speciation and extinction rates may be driven by frontal shield evolution, I used the Binary State Speciation and Extinction (BiSSE) model previously described by Maddison et al. (2007) as implemented in the diversitree package (FitzJohn 2012) for the R software (R Core Team 2013). The BiSSE model also allows the user to correct for missing taxa in its estimates. This is crucial for trees that are incompletely sampled (FitzJohn et al. 2009). This model assumes all tip species have known and correctly assigned trait values. The BiSSE analysis was run on my larger dataset containing 89 cheilostome taxa. The tree was transformed into a rooted ultra-metric tree with the Ape package for R (Paradis et al. 2004). I used the chronos function also implemented in Ape to create a chronogram based on the obtained tree, where branch lengths represent relative time and where all tips are equidistant from the root. Wall types were generalized into ascophoran and anascan states, to force the dataset to be binary (i.e. malacostega, scruparina, inovicellata & flustrina defined as an anascan frontal wall group, and hippothoomorpha, umbomulomorpha, lepraliomorpa & acanthostega as an ascophoran frontal wall group). This is to allow the BiSSE model to estimate speciation and extinction rates for the two frontal wall types and character transition rates between them parametrically. Parameters in each model were estimated first utilizing maximum likelihood, and the estimated parameters were used as starting priors for a Bayesian mcmc parameter estimation run in order to get statistical data. The ML search in BiSSE only returns single data points as estimates, running data through the Bayesian framework allows the user to better explore parameter space. 10.000 inferences were run and the first 2000 inferences discarded as burn-in, as recommended (FitzJohn 2012). Multiple models, including those where speciation and extinction rates for anascans and ascophorans were constrained to be the same or different were explored (table 4). Only nested sequential models can be compared directly in BiSSE, therefore, I used the difference in AIC scores as a criterion for support of one model over another (Burnham and Anderson 2004). In addition, striving to minimize impact of taxon sampling, estimates of sampling rates have been incorporated in the model. In my dataset I estimated a sampling frequency on the generic level (13.5 percent of anascans and 6.5 percent of ascophorans) represented based on Gordon (2009).

Table 3: Model comparison and parameters in BiSSE.

Parameters in BiSSE based on a single binary trait:	
λ_0 --> speciation rate associated with state 0 = "anascan"	
λ_1 --> speciation rate associated with state 1 = "ascophoran"	
μ_0 --> extinction rate associated with state 0 = "anascan"	
μ_1 --> extinction rate associated with state 1 = "ascophoran"	
q_{01} --> transition from 0 "anascan" to 1 "ascophoran"	
q_{10} --> transition from 1 "ascophoran" to 0 "anascan"	
Model 1	Includes all parameters
Model 2	Speciation rates constrained ($\lambda_0 = \lambda_1$)
Model 3	Extinction rates constrained ($\mu_0 = \mu_1$)
Model 4	Transition rates constrained ($q_{01} = q_{10}$)
Model 5	Extinction rates set to 0 ($\mu_0 = \mu_1 = 0$)
Model 6	Transition only from Anasca to Ascophora ($q_{10} = 0$)
Model 7	Transition only from Anasca to Ascophora and no extinction ($q_{10} = 0$, $\mu_0 = \mu_1 = 1$)

To infer ancestral morphologies, I used the MuSSE model, an extension of the BiSSE model where multiple traits can be used instead of one binary trait. I used the ML tree of the large dataset and dropped the Phylactolaemata and outgroup species. This resulted in a tree with 116 taxa. This time, I allowed all species to retain their true frontal wall type, and defined all non-cheilostomes as its own group, resulting in 9 different character states. The reason I chose to retain ctenostomes in this analysis is because they share a MCRA with cheilostomes and this would better allow me to infer when the different shield types evolved. I conducted parameter estimation using ML. I constrained all extinction rates to 0, and all transition rates to be equal. The reason for this is that the full model has nine different extinction rates, speciation rates and a 9x9 transition matrix, which are too many parameters to fit given the size of the dataset.

2.5 Fossil calibration

I used FDPPDiv version 1.3 (Heath et al. 2012) to calibrate node ages with fossil occurrences, in order to infer information on when important splits occurred in Bryozoa. FDPPDiv uses a fixed and rooted tree together with fossil occurrence data to run a Dirichlet Process Prior (DPP) model to estimate node divergence times (Heath et al. 2012). I discarded the 6.000 first iterations as burn-in and ran the model for 100.000 iterations of mcmc sampling saving every 100th iteration. Maximum clade credibility trees were saved with means and 95% highest

posterior density in TreeAnnotator v1.6.1 (Drummond and Rambaut 2007). The importance of motivating parameter choice when it comes to fossil estimates has been highlighted (Heath et al. 2014). I chose to use FDPPDiv as this program uses a fossilized birth-death (FBD) process, which acts as a prior for divergence time dating. This model does not require prior calibration densities, which can have a major impact on the prior and posterior of calibration times (Warnock et al. 2012). Parameters were set to a strict molecular clock. Six fossil occurrences with time estimates where implemented into the model. The base of the phylum is estimated at 540 mya based on the earliest unequivocal fossils of bryozoans and the MRCA of the Cheilostomata order estimated at 155 mya (Taylor 1981, Taylor 1994). Within the stenolamates the MCRA of the genus *Crisia* was set to 135 mya, and the base of the genus *Hornera* at 56 mya (Smith et al. 2013). Within the Cheilstomata order, the MCRA of Electridae was set to 70 mya (Taylor and McKinney 2006), and the MRCA of *Microporella* at 23 mya (Taylor and Mawatari 2005).

3 Results

3.1 Alignment

A total of 87 new sequences were successfully obtained from 27 species (table 4). Two datasets were produced each with 2868 positions (2155 nucleotide and 713 amino acid positions). Dataset One allowing 70% missing data per taxon includes 134 species. Dataset Two allowing 60% missing data per taxon includes 111 species. Visual inspection of the trees showed that the datasets with 80 & 90% missing data were considerably lower supported by bootstrap values, but also that removing more than this (i.e. 50% missing positions and below) did not increase robustness, indicating that the 60/70% missing data mark is optimal for this dataset. This is in concordance with an analysis on the impact of missing data on phylogenies by Wiens and Moen (2008). I excluded a total of 49 gene sequences based on RogueNaRok output (see Appendix 1 table A1) which means they were unstable in the single gene ML inferences. Unstable single genes will decrease statistical support in a concatenated phylogeny.

3.2 Phylogenetic analyses

MrBayes ran for 60 million generations before converging for Dataset Two. Bayesian analysis for Dataset One did not reach convergence. The phylogenetic tree based on Dataset One includes 14 phylactolaemates, 20 stenolaemates, and 96 gymnolaemates and represents the highest taxon representation of any molecular bryozoan phylogeny to date. Both datasets include 15 species which have been newly sequenced during this study (Appendix 3 figure A3.2). The phylogenetic tree based on Dataset Two includes 14 phylactolaemates, 20 stenolaemates, and 73 gymnolaemates, and will be presented here in the main text (figure 2), as this dataset did reach convergence. According to the results of the Icong index (Icong = 5.296, P-value = 1.805e-44) the maximum likelihood inference and Bayesian inference trees are congruent. I consider the following support values based on posterior probability (PP) and bootstrap percentage (BP): Full support 1.00 PP/100 BP, high support >.99 PP/ 90 BP, moderate support >.95 PP/ >65 BP and low support >.90 PP/>50 BP. Support values will be given in posterior probabilities and bootstrap percentage as such: (PP/BP). There is a clear distinguishable monophyletic grouping of the three major classes. The split between

Phylactolaemata and Stenolaemata has high support (1.00/ 96) and the split between Stenolaemata and Gymnolaemata has full support. Within the gymnolaemates there is no support in the split between the Cheilostomata and Ctenostomata orders, although they do emerge as two different clades as expected

Table 4: Overview of sequences generated in this study. The third to eighth columns are genes and those successfully generated in this study are marked with an "X"

Species	ID	ssrDNA/18S	rrnL/16S	rrnS/12S	cox1	cox3	cytb
Adeonellopsis sp. (?)	AW301	X	X	X			X
Aimulosia marsupium	AW725	X	X				X
Akatopora circumsaepta	AW527	X	X			X	
Arachnopusia unicornis	AW293	X	X			X	X
Beania magellanica	AW403	X	X		X	X	
Calwellia gracilis	AW632	X	X	X			
Cellaria sp.	AW532	X	X		X		X
Crassimarginatella	AW519	X	X	X	X	X	X
Crepidacantha zelanica	AW664	X	X	X	X		X
Cupuladria sp.	AW817	X	X	X			X
Dimetopia cornuta	AW631	X					
Euthyroides yellyae	AW533	X	X		X	X	X
Figularia mernae	AW440a	X					
Figularia sp.	AW596	X			X		
Galeopsis sp.	AW580	X	X		X		X
Gephyrotes nitidopunctata	AW187	X		X			X
Hippomenella sp.	AW275	X	X				X
Margaretta barbata	AW514	X	X				X
Micropora sp.	AW592	X	X			X	X
Odontionella Cyclops	AW279	X	X		X		X
Opaeophora lepida	AW733	X	X				
Osthimosia socialis	AW377	X					
Otionella sp.	AW607	X	X	X	X		X
Phaeostachys sp.	AW162	X	X		X		X
Rhynchozoon sp.	AW675						X
Steginoporella sp.	AW730	X	X				X
Synnotum aegyptiacum	AW442						X

Figure 2: Phylogenetic tree of 111 species and 2868 characters. Topology shown is inferred with MrBayes. Node values represent Bayesian Posterior Probabilities/ Bootstrap Percentage (PP/BP) and dashes represent values falling under the cut-off for low support (<90 PP/<50 BP). Scale bar indicates expected substitutions per site per branch length. Taxa with AW-codes are newly sequenced taxa except for the taxa marked with an asterisk which are from an unpublished study by Enevoldsen (2016).
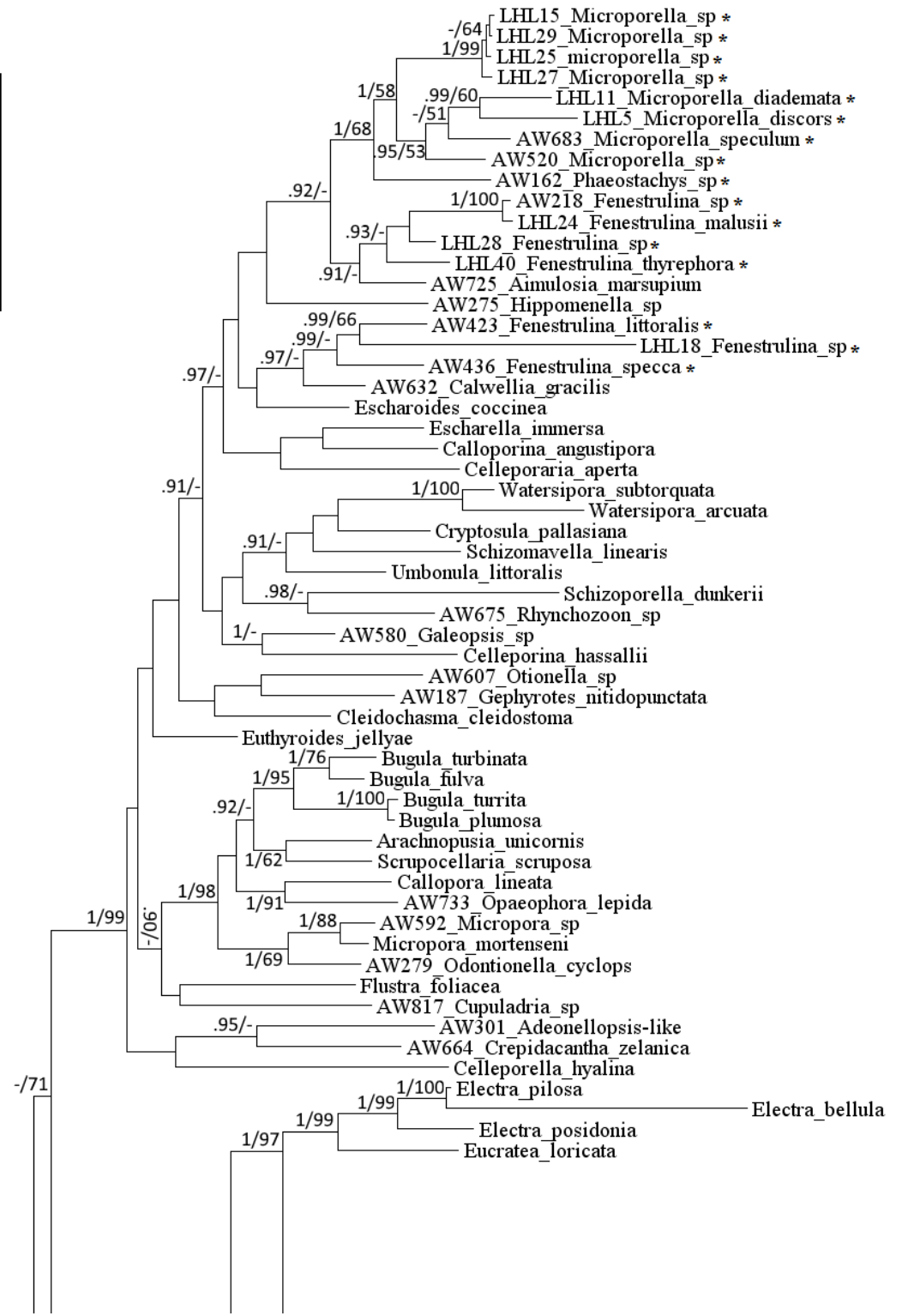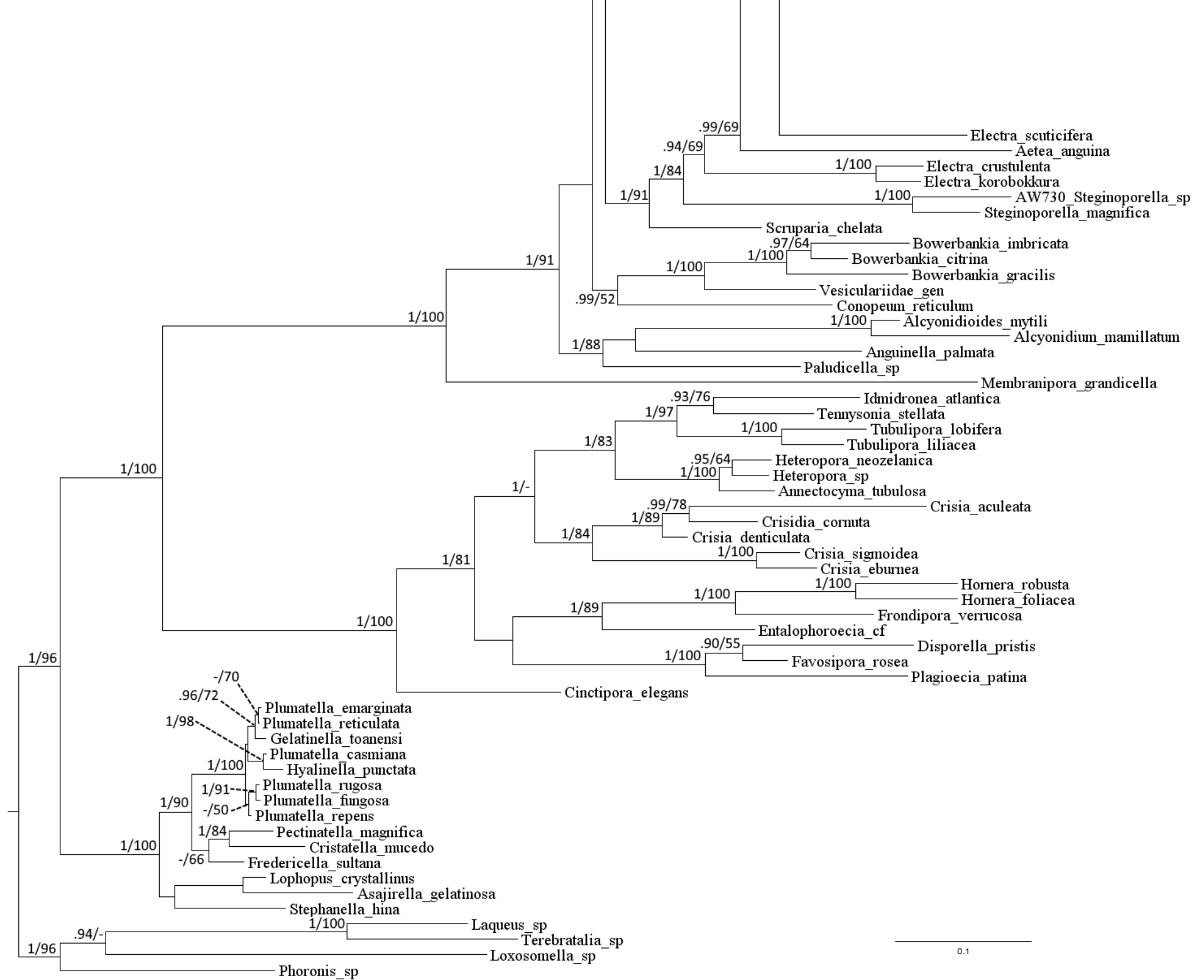
Within the Phylactolaemata six families are recognized, all within the same (and only extant) order Plumatellida: Cristatellidae, Fredericellidae, Lophopodidae, Pectinatellidae, Plumatellidae, and Stephanellidae (Hartikainen et al. 2013). In this study Stephanallidae + Lophopodidae come out as the most basal clade with full support. The split between the two families has moderate bootstrap support, however, it is not supported by posterior probabilities (-/83). Pectinatellidae, Cristatellidae and Fredericellidae are each represented by one species and group together with high support (1.00/90), forming a sister group to Plumatellidae. Plumatellidae as a monophyletic clade has full support.

Within the stenolaemates five extant suborders are recognized: Tubuliporina, Articulata, Cerioporina, Rectangulata, and Cancellata (Boardman 1998). Cinctiporidae emerged as the most basal of the stenolaemates with full support. The Tubuliporina suborder comes out as polyphyletic. Plagioeciidae as a family is polyphyletic with the two representative species not grouping together. Crisiidae, the only family representing the suborder Articulata is monophyletic with moderate bootstrap support and full posterior probability support (1.00/84). The suborder Cancellata represented by family Horneridae is placed with full support next to Frondiporidae. Together with the displaced species *Entalophoroeci*a cf. *robusta* (1.00/ 89) (Plagioeciidae, suborder Tubuliporina) they form a sister group to a group including Licheniporidae (suborder Rectangulata), Densiporidae (suborder Cerioporina) and the other member of Plagioeciidae, although this split is not statistically supported. Family Tubuliporidae (suborder Tubuliporina) is represented by four species and is monophyletic with high support (1.00/97). Family Heteroporidae (Suborder Cerioporina) together with family Annectocymidae (suborder Tubuliporina) are fully supported and form a sister group to family Tubuliporidae (1.00/83).

Within the gymnolaemates Ctenostomata and Cheilostomata do not form monophyletically groups in this tree. Two cheilostomes do not nest within their respective order. With full support, Membraniporidae is placed as the most basal lineage of all gymnolaemates, separate from the other cheilostomes. *Conopeum reticulum* (Family Electridae) is placed within the ctenostomes (.99/52). Eight superfamilies are recognized within Ctenostomata (Bock and Gordon 2013). The order Ctenostomata constitutes of four families in this tree, all within separate suborders. Alcyonidiidae comes out as a monophyletic group, fully supported, forming a sister group to Nolellidae, not supported, which in turn is a high supported sister to Paludicellidae (1.00/88). The remaining family Vesiculariidae is

18

monophyletic with full support. They form a sister group to *Conopeum* (family Electridae, Cheilostomata) (.99/52).

Apart from *Membranipora grandicella* and the two *Conopeum* species (family Membraniporidae and Electridae respectively, both malacostegan families), Scrupariidae (*Scruparia Chelata*) comes out as the most basal lineage of the cheilostome order with high support (1.00/91). It is a sister species to Steginoporellidae which is in turn inferred as the sister group to Electridae (1.00 / 84). Electridae forms a polyphyletic clade to the inclusion of Aeteidae (*Aetea anguina*) and Eucrateidae (*Eucratea loricata),* with the exclusion of the two *Conopeum* taxa. The backbone of the phylogenetic tree has been well supported up until this point. Within the cheilostome order, we find a cluster of neocheilostomes which have overall low support. Neocheilostomatida is an unofficial grade in which all brooding cheilostomes are placed. Hippothoidae is placed monophyletically with two newly sequenced taxa, although this is not statistically supported. AW301 (most likely Adeonidae, unconfirmed) and *Crepidacantha zelanica* (Crepidacanthidae) are placed together (.95/-). Note that species following an AW code described from here on are newly sequenced taxa from this study (NB: not all AW codes in figure 2 are from this study, please refer to figure 2 descriptions). Cupuladriidae (AW664 *Cupuladria sp.*), a family never included in a bryozoan phylogenetic analysis previously, and *Flustra foliacea* (Flustridae, only representative in this study of superfamily Flustroidea) are placed together, although without support. *Micropora mortenseni* & AW592 *Micropora* sp. (both family Microporoidea) come together with good support (1.00/88). They form a sister to another newly sequenced species AW279 *Odontionella Cyclops* (Family Otionellidae) (1.00/69). The two aforementioned families form a sister clade (1.00/98) to a clade including Buguloidea (multiple *Bugula sp.*), Arachnopusiidae (*Arachnopusia unicornis*), Candidae (*Scrupocellaria scruposa*), Microporoidea (AW733 *Opaeophora lepida)*, and Calloporidae (*Callopora lineata*). Family Euthyroidae (*Euthyroides jellyae*) comes out alone with no support yet is placed the same in both trees. Cleidochasmatidae (*Cleidochasma cleidostoma*), Otionellidae (AW607 *Otionella sp.*) and Cribrilinidae (AW187 *Gephyrotes nitidopunctata*) group together in both the ML and Bayesian trees without any satisfactory statistical support. Celleporidae is represented by two species, *Celleporina hassallii* and AW580 *Galeopsis sp.* which group together (1.00/-). Family Phidoloporidae (AW675 *Rhynchozoon sp.*) is a sister to Schizoporellidae (*Schizoporella dunkerii*) (.98/-). Umbonulidae (*Umbonulla littoralis*), Bitectiporidae (*Schizomavella linearis*), Cryptosulidae (*Cryptosula pallasiana*) and the two representatives

of Watersiporidae form a clade. This is not supported well as only Umbonulidae branching off with the rest (.91/-) is supported as well as full support among the two Watersipora species. Family Escharellidae (*Escharella immerse*), *Calloporina angustipora* (Microporellidae) and Lepraliellidae (previous Celleporariidae; *Celleporaria aperta*) group together (.97/-). Romancheinidae (*Escharoides coccinea*) forms a sister to AW632 *Calwellia gracilis* (Family Calwelliidae) without support, which in turn emerges as a sister to three species of genus Fenestrulina (Microporellidae)(.97/-). AW275 *Hippomenella sp.* (not supported), AW162 *Phaeostachys sp.* (1.00/68) both genera from the Escharinidae family together with AW725 *Aimulosia marsupium* (Family Buffonellodidae) (.91/-) all nest within the Microporellidae family. Within Microporellidae, *Microporella* forms a monophyletic genus (1.00/58), while *Fenestrulina* is paraphyletic.

3.3   Statistical analyses in BiSSE

The best model of frontal shield evolution was the model where anascans and ascophorans have different speciation and extinction rates but where transition rates from anascan to ascophoran states and vice versa are constrained to be equal (table 3). The difference in model fit for the next best model was extremely small. In fact, the two best highest scoring models are essentially non-distinguishable if we use the criterion of two delta AIC units as a rule of thumb (Burnham and Anderson 2002). Model 4 has the best fit with an AIC score of -41.276, closely followed by model two which scores -41.124. Model 3 and 1 falls just outside of the two delta AIC score differential. All other models have considerably lower scores (table 5). Ascoporan speciation rates are consistently higher compared to anascan speciation rates, regardless of the specifics of the mode (figure 3). Transition rates are inferred with much higher confidence for anascan to ascophoran transition than vice versa. BiSSE uses the derivative of the maximum likelihood function in a given point in time to infer instantaneous rates. The numbers are scaled after the length of the tree, and are thus best simply interpreted relative to one another.

Table 5: Comparing models of frontal shield evolution. Degrees of freedom (Df column 2), Log Likelihood (lnLik) and Akaike Information Criterion (AIC) output for BiSSE calculated based on the models (column 1) and models are ranked from best (1) to worst (6).

Model	Df	lnLik	AIC	Score
(1) Full model	6	24.600	-37.200	4
(2) Equal speciation	5	25.562	-41.124	2
(3) Equal extinction	5	24.568	-39.136	3
(4) Equal transition	5	25.638	-41.276	1
(5) No extinction	4	20.482	-32.964	5
(6) No q10	5	19.124	-28.247	6
(7) No ext. no q10	3	12.081	-18.162	7

Figure 3: Parameter estimates based on a Bayesian approach using BiSSE. First column: lambda0= speciation rate associated with anascan frontal wall composition. lambda1= speciation rate associated with ascophoran frontal wall composition. Second column: mu0 and mu1= extinction rates associated with anascan and ascophoran frontal walls, respectively. Third column: Transition rates from q01=anascan wall to ascophoran wall and q10=ascophoran wall to anascan wall. All vertical lines represent median values. 95% densities are coloured. Model numbers follow Table 3. Figure continues on the next page.
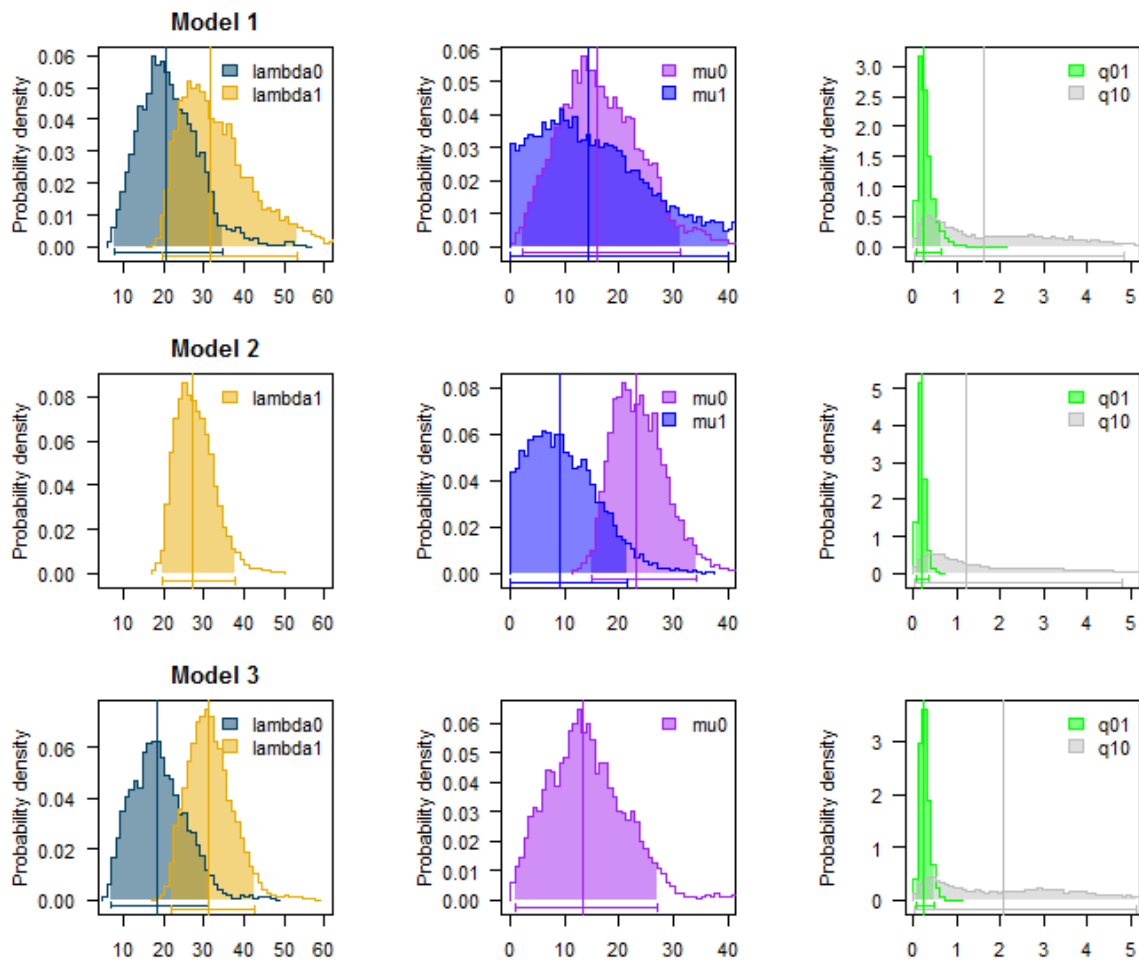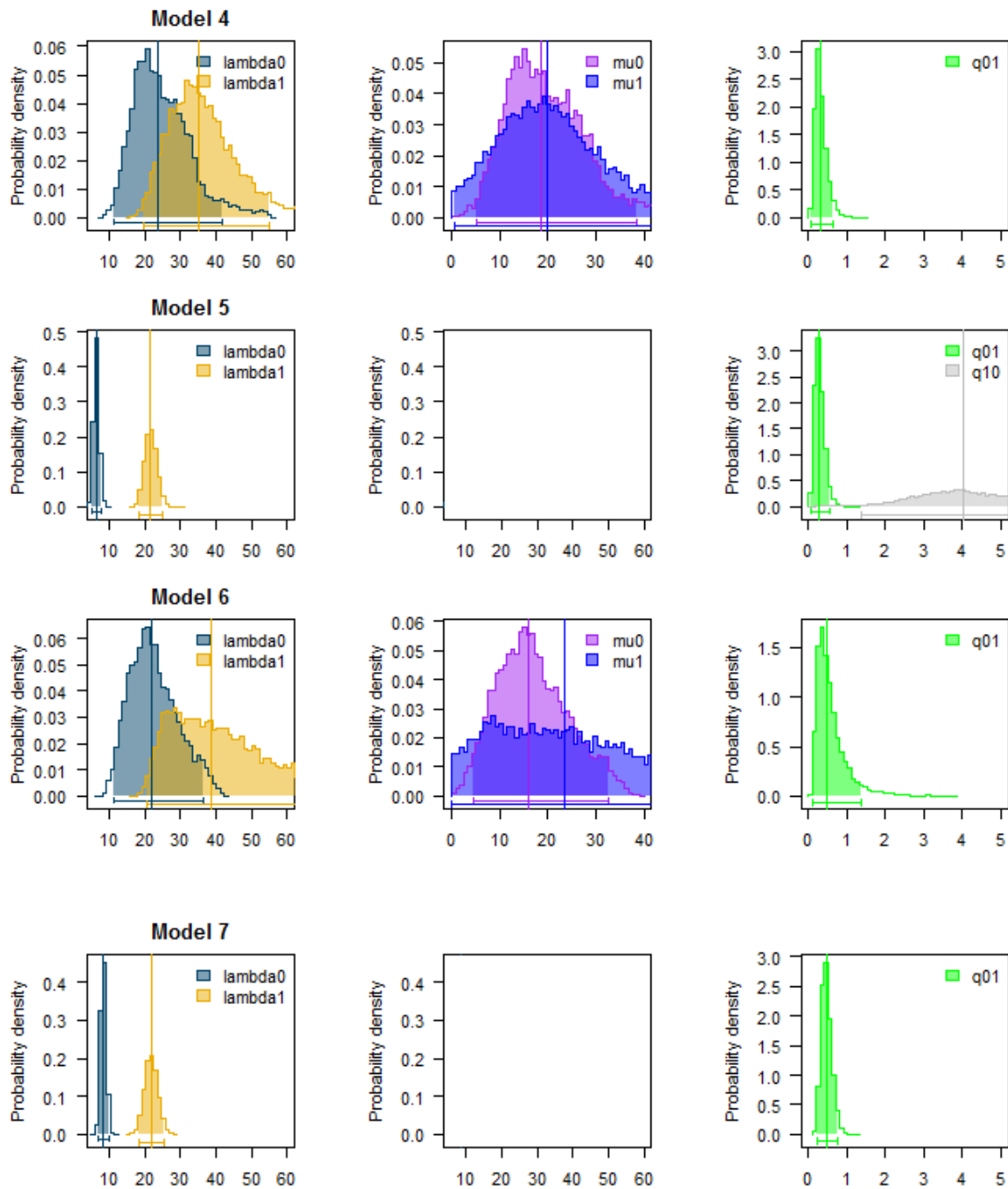
3.4 Ancestral reconstruction in MuSSE

The MuSSE model infers speciation, extinction and transition rates similarly to the BiSSE model, but with multiple traits. Based on the ML inferred parameter estimations (App. Table 4), likely ancestral states can be inferred at the nodes. The ancestral state reconstruction places Malacostina as the oldest frontal wall type (figure 4). This could have been influenced by the placement of *Membranipora grandicella* (a cheilostome) as a sister taxon to

ctenostomes in this phylogony. For this reason, I have conducted ancestral reconstructions in MuSSE both with and without *M. grandicella*. When *M. grandicella* is omitted there is no perceivable change in the ancestral reconstruction, and therefore I only present one figure here. Flustrina is inferred to evolve from either Inovicellata or Malacostega. Lepraliod frontal walls evolved likely from acanthostegan ancestors based on this reconstruction. Acanthostegans could have evolved from either Flustrina or Hippothoomorpha. Umbomulomorpha has evolved multiple times from lepraloids in this analysis, but also twice from Flustrina. The two Scruparina species closely related to the Electridae are not together. This means that in this particular reconstruction Scruparina frontal wall evolved twice. The node, which splits all four hippothoomorpha species, is equally likely to have been Flustrina, Acanthostega or an early Hippothoomorpha, in which case they would have evolved from malacostegans or ctenostome ancestors.

Figure 4: Ancestral reconstruction of frontal wall types; inferred ancestral frontal wall types based on a reconstruction done in MuSSE. Calculations and figure produced in R. Colour codes below.

Membranipora grandic
Alcyonidium mamillat
Alcyonidioides mytil
Anguinella palmata
Paludicella sp
Scruparia chelata
Electra arctica
Electra crustulenta
Electra korobokkura
Eucratea loricata
Electra pilosa
Electra bellula
Electra posidonia
Electra verticillata
Electra scuticifera
Aetea anguina
AW730
Steginoporella magni
Bowerbankia imbricat
Bowerbankia citrina
Bowerbankia gracilis
Vesiculariidae gen
Conopeum seurati
Conopeum reticulum
Micropora mortenseni
AW592
Calyptotheca immersa
Arachnopusia unicorn
Scrupocellaria scrup
Eurystomella foramin
Callopora lineata
AW733
Chaperiopsis lanceol
Beania plurispinosa
Chorizopora brongnia
Bugula turbinata
Bugula fulva
Bugula plumosa
Bugula turrita
Bugula neritina
AW279
Chaperiopsis rubida
Flustra foliacea
AW817
Celleporaria nodulos
Schizoporella dunker
Rhynchozoon zealandi
AW675
Phidoloporidae sp
Crepidacantha crinis
Umbonula littoralis
Watersipora arcuata
Watersipora subtorqu
Smittina torques
Cryptosula pallasian
Schizomavella linear
Smittina rosacea
AW580
Celleporina hassalli
Calloporina angustip
Celleporaria aperta
Escharella immersa
AW275
Hippomenella vellica
LHL28 Fenestrulina s
AW218 Fenestrulina s
LHL24 Fenestrulina m
LHL40 Fenestrulina t
AW725
AW162
AW520 Microporella s
LHL5 Microporella di
LHL11 Microporella d
AW683 Microporella s
LHL27 Microporella s
LHL29 Microporella s
LHL15 Microporella s
LHL25 microporella s
Exochella tricuspis
AW632
AW423 Fenestrulina l
LHL18 Fenestrulina s
AW436 Fenestrulina s
Escharoides angela
Margaretta barbata
Escharoides coccinea
AW187
AW664
Cleidochasma cleidos
AW607
AW301
Euthyroides jellyae
Celleporella hyalina
Antarctothoa bathama
Antarctothoa delta
Antarctothoa tongima

Legend

	Ctenostomata
	Hippothoomorpha
	Lepraliomorpha
	Umbomulomorpha
	Flustrina
	Malacostega
	Inovicellata
	Scruparina
	Acanthostega/cribrimorpha

3.5 Fossil calibration

Fossil calibration has been done on the Bayesian phylogenetic inference of Dataset Two (Appendix figure A3.1). The earliest branches however (i.e. the splits between the three bryozoan classes) remained close to the estimated minimum age estimates. The younger nodes were in some cases estimated to arise a multitude of 4 times earlier than estimates in the paleontological literature. Because of the uncertainty of many nodes in the tree I have subjected to fossil calibrations and because some younger nodes were inferred to be much older than likely given paleontological data, I do not further discuss these results here or use these estimated dates to infer when shield types evolved in absolute time.

4   Discussion

This study has inferred a phylogeny based on sequence data using the largest number of taxa of bryozoans to date. I have used this phylogeny as the basis for investigating several phylogenetic and trait related hypotheses/questions. The variable certainty within my tree allowed me to answer some questions with greater certainty and other with less. Some parts of the discussion are more speculative due to low statistical support for some nodes or a deficiency of tip species. My dataset builds on and further extends the data used in Waechenbach et al. 2012 and hence explicit comparisons will be made between my inferences and those in the aforementioned paper. While the new tree presented here is largely consistent with previous inferences, there are some interesting new relationships proposed nonetheless. An important aspect of this study is to infer where newly sequenced species are placed among previously sequenced cheilostomes.

4.1   Taxonomy, phylogeny and the evolution of brooding

I will first briefly present Stenolaemata. Five taxa have been omitted in my study compared with Waeschenbach et al. (2012). And although the topology is nearly the same, there is one major difference. *Cinctipora elegans* comes out as the most basal lineage, being a sister to all the other stenolaemates (figure 2). This placement is fully supported by both bootstrap values form a maximum likelihood approach and Bayesian posterior probabilities in my analyses. This is very interesting because this family has not been placed unambiguously in a phylogenetic hypothesis despite two previous attempts (see (Waeschenbach et al. 2009, Waeschenbach et al. 2012)). The robust placement in my analysis can be for two reasons. Firstly, the cytb sequence used in the Waeschenbach et al. (2012) was removed in this study based on RogueNaRok output (GenBank accession number JN680897) so this particular sequence might have interfered with the analysis in the previous study. Secondly, multiple taxa previously included were omitted because only 18S sequences were available and as such the data requirement was not met (<40% positions in Dataset Two). In Waeschenbach et al. (2012) large nuclear ribosomal subunit (28S/lsrDNA) sequences were also included for these (and other) species. Species with only nuclear ribosomal sequence data available (i.e. 28S and 18S) have been removed in my dataset. Sequences have been translated into amino acid data as described in the materials and methods, and this could have increased the

phylogenetic signal compared to the Waeschenbach et al. (2012), which used nucleotide sequences for protein coding genes.

Within the Gymnolaemata class the Ctenostomata part of the tree is very much as expected compared to previous phylogenetic inferences. The Cheilostomata part of the tree has multiple clades forming with good support. Family Microporellidae is a controversial grouping and the monophyly of the family has been debated. *Microporella* is monophyletic in my tree. Four newly sequenced species are inferred to be closely related to the Microporellideae family. The first is AW632 *Calwellia gracilis* (Calwelliidae). Calwelliidae has been thought to be closely related to Microporellidae based on structural similarities in both genera (Gordon 1984). It emerges as a sister to *Fenestrulina* which supports this theory. The second species is AW162 *Phaeostachys sp.* which placement is as a sister taxon to *Microporella*. The last two newly sequenced species are AW275 *Hippomenella sp.* & AW725 *Aimulosia marsupium* (Family Buffonellodidae, another family not included in a phylogenetic hypothesis previously). All four species and Microporellidae belong to the Schizoporelloidea superfamily. Flustrina as a grade it not monophyletic as it is interspersed with other species. All newly sequenced Flustrina grade species do emerge within this grade, as expected. AW592 *Micropora sp.* is grouped with *Micropora mortenseni* (Family Microporoidea). The newly sequenced species AW279 *Odontionella cyclops* (Family Foveolariidae, which has not been included in a phylogenetic study before) is placed as a sister species to Microporoidea. AW733 *Opaeophora lepida* and AW817 *Capuladria sp.* are both inferred to belong to the same clade as the species mentioned above.

Stegionoprorella nests within the same clade as *Aetea anguina*, *Scruparia chelata* and Electridae. Ostrovsky (2013) notes that the findings in Knight et al. (2011) indirectly confirm the independent origins of thalamoporellids, which are closely related to steginoporellids, from the other neocheilostomes. The phylogeny presented here lends credit to this hypothesis. The two *Steginoporella* specimens are placed robustly as a sister to Electridae. Malacostegans which are thought to have the most plesiomorphic wall type in Cheilosomata have no brooding of larvae. They have free living cyphonaut larvae which are released into the water column, where they feed and eventually establish a new colony. Cheilostome brooders on the other hand keep their larvae in brooding chambers, where they grow from nutrition obtained from the colony (lecithotrophic larvae). The findings presented here support the hypothesis that brooding cheilostomes evolved at least twice within the order with high certainty.

Within the cheilostomes the statistical support is very low for parts of the tree. Taxon sampling has been proposed to be more important than molecular sampling when attempting to improve statistical support for a tree (Zwickl and Hillis 2002), and I highlight the need for more cheilostome species to be sequenced. One reason for the low support within the cheilostomes could be due to the early radiation of the group. Relatively long evolutionary times after a major radiation can potentially mask phylogenetic signals of a clade. *Conopeum* (Electridae) is placed as a sister to Vesiculariidae which is problematic. *Conopeum* is a malacostegan genera within the Electridae family, and should be placed accordingly. Another point of interest is *Membranipora grandicella*, another malacostegan which is placed far from where it is expected (at the base of Ctenostomata). I expect both placements to change with more extensive gene sampling.

4.2 Frontal shields evolution and diversification

One aspect of bryozoans that has sparked curiosity is their frontal shields, or lack thereof. Traditionally cheilostomes were divided into Anasca and Ascophora. The anascan clade has since been divided into three suborders Malacostegina, Inovicellina and Scrupariina as well as the infraorder Flustrina. Waeschenbach et al. (2012) included representatives of all four clades and also inferred the non-monophyly of anascans as well as Flustrina being paraphyletic with ascophorans. Scrupariina and Inovicellina are now thought to have evolved from malacostegans (Waeschenbach et al. 2012). Within the ascophoran group there are now four grades recognized based on frontal wall types. These are Acanthostegomorpha, Hippothoomorpha, Umbonulomorpha, Lepraliomorpha. How often the different types have evolved is unclear. Knight et al. (2011) found all four ascophoran grades to be polyphyletic in a genetic study including 91 species. However, monophyly could not be statistically rejected for Hippothoomorpha and a combined clade of Umbonulomorpha and Lepraliomorpha (Knight et al. 2011). All four ascophoran grades are also found to be polyphyletic in this study. One hypothesis that still stands is that of multiple umbonulomorphic origins of Lepraliomorpha (Knight et al. 2011). Lepraliomorpha and Umbonulomorpha form one big clade to the exclusion of two species, which nest in other parts of the tree. They are *A. Unicornins* (umbonulomorph) + *Calyptotheca immerse* (lepraliomorph) and are both inferred to have evolved from Flustrina. The former was placed similarly in Knight et al. (2011). My

dataset supports the idea that there are multiple origins of Umbonulomorpha from Lepraliomorpha. The ancestral reconstruction results presented in figure 4 must be viewed as preliminary because of the low statistical support for the tree and the fact that the MuSSE ancestral reconstruction might not be the most optimal method for ancestral reconstruction, as it is a model mainly intended for inferring rates of speciation, extinction and transition.

In all models tested in the BiSSE environment, ascophorans have a higher speciation rate relative to anascans. In the highest scoring model where extinction rates are forced to be different, the extinction rates are nevertheless very similar for the two grades. The next best model has speciation rates constrained, in which case the data is fitted with a much higher relative extinction rate for anascans. I note here it is well known that inferring extinction rates based on molecular phylogenies inferred from extant species only is often problematic (Rabosky 2010). Parameter values often approach zero, and in this study we see the same trend. Specifically for BiSSE, speciation rates are estimated with much higher statistical accuracy than extinction rates (Maddison et al. (2007)). Transition rates for q10 are much higher relative to q01 in all models where different rates as estimated, which contrasts somewhat with the ideas persistent in the literature that ascophorans have arisen multiple times from anascan ancestors (McKinney and Jackson 1991, Dick et al. 2009), but not vice versa, hence begging further research.

There are four caveats to BiSSE analyses as applied here. The first is the sampling in my tree. As stated in the methods, the model can accommodate varying sampling frequencies of the two states (frontal shields in this case). However, the sampling frequencies for both of these states were both very low, compared to the true species diversity of these grades (43 genera out of 1049 as currently accepted by Gordon 2009). While FitzJohn et al. (2009) argued that incompletely sampled trees may be used in BiSSE analyses, given that sampling is random with respect to the morphological traits we are interested in, that might not apply here: I have sampled multiple species of several families, and one or none of many other families. Microporellidae, Electridae and Buguloidea are examples of clades represented by multiple species.. Secondly, the BiSSE model assumes the tree used in the analysis to be correct. As stated before, statistical support is low, or completely non-existing for parts of the cheilostome subtree. Third, the model accommodates only two states, capturing only broad similarities among frontal shield grades, while we know there is much more variation which to an extent can be appreciated from more finally divided grades such as umbomulomorpha,

lepraliamorpha etc. And although the MuSSE model could be used for such inferences, it is not possible with my data because of point one (low taxonomic sampling). Fourth, the possibility of confounding effects cannot be accounted for within the scope of this study. I mentioned other morphological traits in the introduction. Ovicells, avicularia, larval types would all be good candidates for a study like this. Traits are known to vary on low taxonomic levels, even within genera. In addition, some morphological traits are not adequately described in the literature. A comparison across traits therefore proved difficult. As explained in the introduction, there are multiple possible morphological novelties in cheilostomes that could account for the diversification we see in the fossil record. However, despite the possibility of confounding effect and the shortcomings in data sampling, I still believe that the results are interesting. As far as I know, a study that parameterizes speciation and extinction rates based on a trait has not been done before in bryozoans. The preliminary estimates suggest that ascophorans do have a higher diversification rate, be it through a higher speciation rate or a lower extinction rate compared to their anascan counterparts.

4.3 Fossil analysis

It has been problematic to infer absolute timing of speciation events from molecular data alone. One of the challenges with calibrating a phylogenetic tree to absolute time has been overcoming the cumbersome fact of substitution rate variation. Especially in larger datasets with a clade history far back in time, it is common for different lineages to have different substitution rates (Gu et al. 1995). Methods assuming the molecular clock model have therefore been replaced by newer methods that allow branch estimates to be unconstrained under relaxed-clock models (e.g. (Gustafsson et al. 2010, Smith et al. 2010)). Relaxed clock models are used in combination with models estimating how distributions of speciation events happen over time. One such model is a birth death model, which I have used in this study. This study only uses few calibration points. The model used for calibration allows for multiple fossil occurrences per lineage. Multiple fossils along lineages and a higher fossil occurrence count in general is more important than extant taxon sampling (Hug and Roger 2007). I highlight the need for a database with scored morphological traits in fossils occurrences of Bryozoa as this would increase the power of studies such as this tremendously.

5 Conclusion

5.1 Conclusion and closing remarks

This research project studied the evolution of bryozoans by inferring phylogenetic relationships and investigating hypotheses of trait evolution. The focus has been on cheilostomes, as this order represents the largest bulk of extant bryozoan species. Through molecular sequencing of new species, I added 15 species that are new to phylogenetic reconstructions of bryozoans. The resulting phylogenetic hypothesis was used in a binary state speciation and extinction model to infer whether there was a difference in rates of speciation among anascans and ascophorans. An attempt has been made to infer absolute time based on fossil occurrences.

Among the newly sequenced species, six families were represented which had not been previously included in a phylogeny. Calwellidae and Foveolariidae have been robustly placed in the new phylogenetic hypothesis. The former is shown to be closely related to Microporellidae and the latter to Microporoidae. The four remaining families Buffonellodidae, Cribrilinidae, Cupuladriidae, and Otionellidae have not been placed robustly. Cupuladriidae was, however, placed together with the other Flustrina species. Steginoporellidae was found to reside within the malacostegan grade. This strengthens the hypothesis that brooding has evolved multiple times independently in cheilostomes. All remaining neocheilostomes formed one clade. The BiSSE analysis performed on anascan and ascophoran frontal shield data gives the indication that acsophorans have a higher net diversification rate compared to anascans. These results are only preliminary. More data needs to be included in order to properly carry out such an analysis. In the future, the larger grades which together form anascans and ascophorans will have to be analysed separately. Also, the effect of confounding effects needs to be explored, and traits other than frontal walls need to be used in the same analytic setting.

While many questions remained unanswered, this thesis is one more step towards a better understanding of bryozoan evolution and also demonstrated the utility of evolutionary models such as BiSSE in understanding morphological evolution and diversification among bryozoans with different traits.

References

Altschul, S. F. (1998). "Generalized affine gap costs for protein sequence alignment." Proteins Structure Function and Genetics **32**(1): 88-96.

Altschul, S. F., W. Gish, W. Miller, E. W. Myers and D. J. Lipman (1990). "Basic local alignment search tool." Journal of molecular biology **215**(3): 403-410.

Benson, D. A., M. Cavanaugh, K. Clark, I. Karsch-Mizrachi, D. J. Lipman, J. Ostell and E. W. Sayers (2013). "GenBank." Nucleic Acids Res **41**(Database issue): D36-42.

Bergsten, J. (2005). "A review of long-branch attraction." Cladistics **21**(2): 163-193.

Boardman, R. S. (1998). "Reflections on the morphology, anatomy, evolution, and classification of the Class Stenolaemata (Bryozoa)."

Bock, P. E. and D. P. Gordon (2013). "Phylum Bryozoa Ehrenberg, 1831. In: Zhang, Z.-Q.(Ed.) Animal Biodiversity: An Outline of Higher-level Classification and Survey of Taxonomic Richness (Addenda 2013)." Zootaxa **3703**(1): 67-74.

Burnham, K. and D. Anderson (2002). "Information and likelihood theory: a basis for model selection and inference." Model selection and multimodel inference: a practical information-theoretic approach: 49-97.

Burnham, K. P. and D. R. Anderson (2004). "Multimodel Inference: Understanding AIC and BIC in Model Selection." Sociological Methods & Research **33**(2): 261-304.

Castresana, J. (2000). "Selection of Conserved Blocks from Multiple Alignments for Their Use in Phylogenetic Analysis." Molecular Biology and Evolution **17**(4): 540-552.

Darriba, D., G. L. Taboada, R. Doallo and D. Posada (2011). "ProtTest 3: fast selection of best-fit models of protein evolution." Bioinformatics.

Darriba, D., G. L. Taboada, R. Doallo and D. Posada (2012). "jModelTest 2: more models, new heuristics and parallel computing." Nat Meth **9**(8): 772-772.

de Vienne, D. M., T. Giraud and O. C. Martin (2007). "A congruence index for testing topological similarity between trees." Bioinformatics **23**(23): 3119-3124.

Dick, M. H., S. Lidgard, D. P. Gordon and S. F. Mawatari (2009). "The origin of ascophoran bryozoans was historically contingent but likely." Proceedings of the Royal Society B-Biological Sciences **276**(1670): 3141-3148.

Drummond, A. J. and A. Rambaut (2007). "BEAST: Bayesian evolutionary analysis by sampling trees." BMC Evolutionary Biology **7**(1): 1-8.

Enevoldsen, E. L. G. (2016). "Microporellidae phylogeny and evolution." http://www.duo.uio.no/.

32

FitzJohn, R. G. (2012). "Diversitree: comparative phylogenetic analyses of diversification in R." Methods in Ecology and Evolution **3**(6): 1084-1092.

FitzJohn, R. G., W. P. Maddison and S. P. Otto (2009). "Estimating Trait-Dependent Speciation and Extinction Rates from Incompletely Resolved Phylogenies." Systematic Biology **58**(6): 595-611.

Fuchs, J., M. Obst and P. Sundberg (2009). "The first comprehensive molecular phylogeny of Bryozoa (Ectoprocta) based on combined analyses of nuclear and mitochondrial genes." Molecular Phylogenetics and Evolution **52**(1): 225-233.

Gadberry, M. D., S. T. Malcomber, A. N. Doust and E. A. Kellogg (2005). "Primaclade--a flexible tool to find conserved PCR primers across multiple species." Bioinformatics **21**(7): 1263-1264.

Gish, W. and D. J. States (1993). "Identification of protein coding regions by database similarity search." Nature genetics **3**(3): 266-272.

Gordon, D. P. (1984). The marine fauna of New Zealand: Bryozoa, Gymnolaemata from the Kermadec Ridge, New Zealand Oceanographic Institute.

Gordon, D. P. (2009). "Genera and subgenera of Cheilostomatida. INTERIM Classification (Working

Classification for Treatise)."

Gordon, D. P., P. D. Taylor and F. P. Bigey (2009). " Phylum Bryozoa - moss animals, sea mats, lace corals." The New Zealand Inventory of Biodiversity. **Volume 1. Kingdom Animalia - Radiata, Lophotrochozoa, and Deuterostomia.**: 271-297.

Gu, X., Y.-X. Fu and W.-H. Li (1995). "Maximum likelihood estimation of the heterogeneity of substitution rate among nucleotide sites." Molecular Biology and evolution **12**(4): 546-557.

Gustafsson, A. L. S., C. F. Verola and A. Antonelli (2010). "Reassessing the temporal evolution of orchids with new fossils and a Bayesian relaxed clock, with implications for the diversification of the rare South American genus Hoffmannseggella(Orchidaceae: Epidendroideae)." BMC Evolutionary Biology **10**(1): 1-13.

Hall, T. (2004). "BioEdit version 7.0. 0." Distributed by the author, website: www. mbio. ncsu. edu/BioEdit/bioedit. html.

Hartikainen, H., A. Waeschenbach, E. Woss, T. Wood and B. Okamura (2013). "Divergence and species discrimination in freshwater bryozoans (Bryozoa: Phylactolaemata)." Zoological Journal of the Linnean Society **168**(1): 61-80.

Hausdorf, B., M. Helmkampf, M. P. Nesnidal and I. Bruchhaus (2010). "Phylogenetic relationships within the lophophorate lineages (Ectoprocta, Brachiopoda and Phoronida)." Molecular Phylogenetics and Evolution **55**(3): 1121-1127.

Heath, T. A., M. T. Holder and J. P. Huelsenbeck (2012). "A Dirichlet Process Prior for Estimating Lineage-Specific Substitution Rates." Molecular Biology and Evolution **29**(3): 939-955.

Heath, T. A., J. P. Huelsenbeck and T. Stadler (2014). "The fossilized birth–death process for coherent calibration of divergence-time estimates." Proceedings of the National Academy of Sciences **111**(29): E2957-E2966.

Hillis, D. M. and M. T. Dixon (1991). "Ribosomal DNA: Molecular Evolution and Phylogenetic Inference." The Quarterly Review of Biology **66**(4): 411-453.

Hug, L. A. and A. J. Roger (2007). "The Impact of Fossils and Taxon Sampling on Ancient Molecular Dating Analyses." Molecular Biology and Evolution **24**(8): 1889-1897.

Jackson, J. B. (1985). "Distribution and ecology of clonal and aclonal benthic invertebrates."

Katoh, K. and D. M. Standley (2013). "MAFFT multiple sequence alignment software version 7: improvements in performance and usability." Mol Biol Evol **30**(4): 772-780.

Knight, S., D. P. Gordon and S. D. Lavery (2011). "A multi-locus analysis of phylogenetic relationships within cheilostome bryozoans supports multiple origins of ascophoran frontal shields." Molecular Phylogenetics and Evolution **61**(2): 351-362.

Lidgard, S., M. C. Carter, M. H. Dick, D. P. Gordon and A. N. Ostrovsky (2012). "Division of labor and recurrent evolution of polymorphisms in a group of colonial animals." Evolutionary Ecology **26**(2): 233-257.

Maddison, W. P., P. E. Midford and S. P. Otto (2007). "Estimating a Binary Character's Effect on Speciation and Extinction." Systematic Biology **56**(5): 701-710.

Maddison, W. P. a. D. R. M. (2015). "Mesquite: a modular system for evolutionary analysis. Version 3.04." http://mesquiteproject.org.

McKinney, F. K. and J. B. C. Jackson (1991). Bryozoan Evolution, University of Chicago Press.

Ostrovsky, A. N. (2013). Evolution of sexual reproduction in marine invertebrates: example of gymnolaemate bryozoans, Springer Science & Business Media.

Paradis, E., J. Claude and K. Strimmer (2004). "APE: analyses of phylogenetics and evolution in R language." Bioinformatics **20**(2): 289-290.

Porter, J. S., J. S. Ryland and G. R. Carvalho (2002). "Micro- and macrogeographic genetic structure in bryozoans with different larval strategies." Journal of Experimental Marine Biology and Ecology **272**(2): 119-130.

R Core Team (2013). "R: A language and environment for statistical computing." R Foundation for Statistical Computing **http://www.R-project.org/**.

Rabosky, D. L. (2010). "EXTINCTION RATES SHOULD NOT BE ESTIMATED FROM MOLECULAR PHYLOGENIES." Evolution **64**(6): 1816-1824.

Rambaut, A., M. Suchard, D. Xie and A. Drummond (2014). Tracer v1. 6.

Ronquist, F. and J. P. Huelsenbeck (2003). "MrBayes 3: Bayesian phylogenetic inference under mixed models." Bioinformatics **19**(12): 1572-1574.

Simon, C., F. Frati, A. Beckenbach, B. Crespi, H. Liu and P. Flook (1994). "Evolution, Weighting, and Phylogenetic Utility of Mitochondrial Gene Sequences and a Compilation of Conserved Polymerase Chain Reaction Primers." Annals of the Entomological Society of America **87**(6): 651-701.

Smith, A. M., P. D. Taylor and R. Milne (2013). Hornera striata (Milne Edwards, 1838), a British Pliocene Cyclostome Bryozoan Incorrectly Recorded from New Zealand, with Notes on Some Non-fenestrate Hornera from the Coralline Crag. Bryozoan Studies 2010. A. Ernst, P. Schäfer and J. Scholz. Berlin, Heidelberg, Springer Berlin Heidelberg**:** 339-356.

Smith, S. A., J. M. Beaulieu and M. J. Donoghue (2010). "An uncorrelated relaxed-clock analysis suggests an earlier origin for flowering plants." Proceedings of the National Academy of Sciences **107**(13): 5897-5902.

Taylor, P. (1981). "Bryozoa from the Jurassic Portland beds of England." Palaeontology **24**(Pt 4): 863-875.

Taylor, P. (1994). "An early cheilosteme bryozoan from the Upper Jurassic of Yemen.(With 4 figures in the text)." Neues Jahrbuch fur Geologie und Palaontologie-Abhandlungen **191**(3): 331-344.

Taylor, P. D. (2005). "Bryozoans." Encyclopaedia of geology **2**: 310-320.

Taylor, P. D. and S. F. Mawatari (2005). Preliminary overview of the cheilostome bryozoan Microporella, A.A. Balkema Publishers.

Taylor, P. D. and F. K. McKinney (2006). "Cretaceous Bryozoa from the Campanian and Maastrichtian of the Atlantic and Gulf coastal plains, United States."

Taylor, P. D., A. Waeschenbach, A. M. Smith and D. P. Gordon (2015). "In search of phylogenetic congruence between molecular and morphological data in bryozoans with extreme adult skeletal heteromorphy." Systematics and Biodiversity **13**(6): 525-544.

Waeschenbach, A., C. J. Cox, D. T. J. Littlewood, J. S. Porter and P. D. Taylor (2009). "First molecular estimate of cyclostome bryozoan phylogeny confirms extensive homoplasy among skeletal characters used in traditional taxonomy." Molecular Phylogenetics and Evolution **52**(1): 241-251.

Waeschenbach, A., P. D. Taylor and D. T. J. Littlewood (2012). "A molecular phylogeny of bryozoans." Molecular Phylogenetics and Evolution **62**(2): 718-735.

Warnock, R. C. M., Z. Yang and P. C. J. Donoghue (2012). "Exploring uncertainty in the calibration of the molecular clock." <u>Biology Letters</u> **8**(1): 156-159.

Zwickl, D. J. and D. M. Hillis (2002). "Increased Taxon Sampling Greatly Reduces Phylogenetic Error." <u>Systematic Biology</u> **51**(4): 588-598.

Appendix 1: Taxonomic overview

Table A1.1: species and genes-sequences in this study. Column 1: higher taxonomy/species names. Column 2 through 7: accession codes of the genes used in this study, from left to right; small ribosomal subunit (nuclear), large ribosomal subunit (mitochondrial), small ribosomal subunit (mitochondrial), cytochrome c oxidase subunit 1 (mitochondrial), cytochrome c oxidase subunit 3 (mitochondrial), and cytochrome b (mitochondrial). Species with strikethrough have been omitted from the dataset because of too little data (<30% positions fulfilment as described in the 'Materials and Methods' section). Species followed by an asterisk are one of 23 species only included in Dataset One. Grey coloured codes have been omitted from the dataset based on RogueNaRok output. This study: sequences produces in this study. EE: sequences from Enevoldsen (2016).

Tax. Level/Species	18S	16S	12S	cox1	cox3	cytb
Outgroup						
Loxosomella spp.	AY218100	NC_010432	NC_010432	YP_001718401	NC_010432	YP_001718408
Terebratalia transversa	FJ196115	NC_003086	NC_003086	NP_203506	NP_203509	NP_203507
Laqueus spp.	U083231	NC_002322	NC_002322	NP_058502	NP_058509	NP_058503
Phoronis spp	U36271	AY368231	AY368231	AAR13390	AAR13386	AAR13396
Class Phylactolaemata						
Family Stephanellidae						
Stephanella hina	JN680924	AB365644	AB365621			
Family Lophopodidae						
Asajirella gelatinosa	FJ196126	AB365641	AB365618	ACN91253		
Lophopus crystallinus	JN680925	JN681053	JN681089	ACN91264	AEV21514	AEV21434
Lophopodella carteri		AB365642	AB365619			
Family Fredericellidae						
Fredericella indica		AB365638	AB365615			
Fredericella sultana	JN680926	JN681054	JN681090	AEV21478	AEV21515	AEV21435
Family Cristatellidae						
Cristatella mucedo	AF025947	JN681051	JN681087	ACN91263	AEV21512	AEV21432
Family Pectinatellidae						
Pectinatella magnifica	FJ409600	JN681052	JN681088	AEV21476	AEV21513	AEV21433
Family Plumatellidae						
Gelatinella toanensis	FJ196112	AB365630	AB365607	ACN91239		BAG31922
Hyalinella punctata	JN680927	JN681055	AB365608	AHY02393		BAG31921
Internectella bulgarica		AB365636	AB365613			BAG31924
Plumatella fungosa	JN680928	JN681056	AB365601	AHH29625		
Plumatella emarginata	JN680929	JN681057	JN681091	AEV21479	AEV21516	AEV21436
Plumatella repens	JN680930	JN681058		ACN91262		BAG31913
Plumatella rugosa	JN680931	JN681059	AB365600			BAG31914
Plumatella casmiana	JN680933	JN681063	AB365606	AHY02392		BAG31919
Plumatella minuta		AB365635	AB365612			BAG31923
Plumatella vorstmani		AB365634	AB365611			
Plumatella reticulata	DQ530349	AB365628	AB365605			BAG31918
Plumatella mukaii		AB365627	AB365604			BAG31920
Plumatella fruticosa	KC461940	KC461983				
Plumatella vaihiriae		JN681060	AB36560			BAG31916

Tax. Level/Species	18S	16S	12S	cox1	cox3	cytb
Plumatella geimermassardi	JN68093	JN681062				

Class Stenolaemata

Order CYclostomata

Suborder Articulata
Family Crisiidae

Tax. Level/Species	18S	16S	12S	cox1	cox3	cytb
Crisia aculeata	FJ196134			ACN91260		
Crisia eburnea	FJ152032			ACN91248		
Crisia pseudosolena		KF714809		AHB62238		
Crisia sigmoidea	FJ409608	JN681067	JN681100		AEV21523	AEV21444
Crisia denticulata	FJ409606			AEV21490	AEV21528	AEV21449
Crisidia cornuta	FJ196135			ACN91261		
Crisia fistulosa	FJ409607					
Filicrisia geniculata	FJ152035					

Suborder Cancellata
Family Horneridae

Tax. Level/Species	18S	16S	12S	cox1	cox3	cytb
Hornera robusta	FJ409615			AEV21487	AEV21525	AEV21445
Hornera foliacea	FJ409613	JN681068		AEV21488	AEV21526	AEV21446
Hornera cf. caespitosa	FJ409614					

Suborder Cerioporina
Family Densiporidae

Tax. Level/Species	18S	16S	12S	cox1	cox3	cytb
Favosipora rosea	FJ409605			AEV21491	AEV21529	AEV21450

Family Heteroporidae

Tax. Level/Species	18S	16S	12S	cox1	cox3	cytb
Heteropora sp.	FJ409610		JN681098		AEV21520	AEV21442
Heteropora neozelanica	FJ409609		JN681099	AEV21484	AEV21521	AEV21443

Suborder Rectangulata
Family Licheniporidae

Tax. Level/Species	18S	16S	12S	cox1	cox3	cytb
Disporella pristis	FJ409604		JN681093	AEV21485	AEV21522	
Disporella hispida	FJ409602			FJ196093		
Disporella cf. neapolitana	FJ409603					

Suborder Tubuliporina
Family Diastoporidae

Tax. Level/Species	18S	16S	12S	cox1	cox3	cytb
Diplosolen obelia	FJ409616					

Family Diaperoeciidae

Tax. Level/Species	18S	16S	12S	cox1	cox3	cytb
Diaperoecia purpurascens	KP331440					

Family Annectocymidae

Tax. Level/Species	18S	16S	12S	cox1	cox3	cytb
Annectocyma tubulosa	FJ409619	JN681066	JN681097	AEV21483	AEV21519	AEV21441

Family Frondiporidae

Tax. Level/Species	18S	16S	12S	cox1	cox3	cytb
Frondipora verrucosa	FJ409612			AEV21489		AEV21447

Family Plagioeciidae

Tax. Level/Species	18S	16S	12S	cox1	cox3	cytb
Plagioecia patina	FJ409623		JN681092	ACN91259		AEV21437
Entalophoroecia cf. robusta	FJ409618			AEV21486	AEV21524	
Cardioecia watersi	FJ409617					

Family Tubuliporidae

Tax. Level/Species	18S	16S	12S	cox1	cox3	cytb
Tubulipora flabellaris		EU563937	EU563937	YP_004581394	YP_004581404	YP_004581402

Tax. Level/Species	18S	16S	12S	cox1	cox3	cytb
Idmidronea atlantica	FJ409620	JN681065	JN681096	JN681096	AEV21518	AEV21440
Tennysonia stellata	JF893944			AEV21482		
Tubulipora liliacea	FJ409622		JN681094			AEV21438
Tubulipora lobifera	JN680934	JN681064	JN681095		AEV21517	AEV21439
Family Cinctiporidae						
Cinctipora elegans	FJ409611				AEV21527	AEV21448

Class Gymnolaemata

Order Ctenostomata
Family Alcyonidiidae

Tax. Level/Species	18S	16S	12S	cox1	cox3	cytb
Alcyonidium mamillatum	FJ196130			FJ196100		
Alcyonidium mytili	JN680936	JN681069	JN681102	AEV21493	AEV21531	AEV21452
Alcyonidium sp.	AM886861	AM747493				
Family Flustrellidridae						
Flustrellidra hispida	FJ409601	NC_008192	NC_008192	YP_654707.1	YP_654699.1	YP_654711.1
Family Vesiculariidae						
Amathia sp.		JN681086				AEV21474
Bowerbankia gracilis	JN680938	JN681071	JN681105	AJB84775	AEV21533	AEV21455
Bowerbankia imbricata	JN680939	JN681072	JN681106	AJB84777	AEV21534	AEV21456
Bowerbankia citrina	KM373512	KM373503	JN681121	AJB84771		AEV21473
Bowerbankia n. sp.			JN681104			AEV21454
Vesiculariidae gen. n. sp. N		JN681085	JN681120	AEV21511	AEV21545	AEV21472
Family Nolellidae						
Anguinella palmata	JN680935	KM373501	JN681101	AJB84768	AEV21530	AEV21451
Family Paludicellidae						
Paludicella sp.	JN680937	JN681070	JN681103	AEV21494	AEV21532	AEV21453

order Cheilostomata
Grade Hippothoomorpha
Family Hippothoidae

Tax. Level/Species	18S	16S	12S	cox1	cox3	cytb
Celleporella hyalina	JN680948	JN681079	JN681113	AFJ53903	AFJ53912	AFJ53907
*Antarctothoa tongima**	JF950364	JF950308		AEL29593		
*Antarctothoa delta**	JF950363	JF950313		ABY26230		
*Antarctothoa bathamae**	JF950365	JF950303		AEL29591		
Family Chorizoporidae						
*Chorizopora brongniartii**	JF950366	JF950324		AEL29595		
Family Arachnopusiidae						
Arachnopusia unicornis	JF950378	JF950305		AEL29594		
Family Umbonulidae						
Umbonula littoralis	JN680953	JN681082	JN681116	AEV21508	AEV21542	AEV21469
Family Romancheinidae						
Escharella immersa	FJ196116			AEV21501		AEV21463
Family Exochellidae						
*Escharoides angela**	JF950360	JF950338		AEL29587		
*Exochella tricuspis**	JF950361	JF950341		AEL29599		
Escharoides coccinea	FJ152034			AEV21505		AEV21466

Tax. Level/Species	18S	16S	12S	cox1	cox3	cytb
Grade Lepraliomorpha						
Family Lepraliellidae (previous Celleporariidae)						
Celleporaria aperta	FJ009086	AY789093				
Celleporaria agglutinans	JF950355	JF950310		AEL29617		
*Celleporaria nodulosa**	JF950357	JF950329		AEL29609		
Superfamily Smittinoidea						
Family Smittinidae						
*Smittina rosacea**	JF950377	JF950318		AEL29603		
*Smittina torques**	JF950375	JF950352		AEL29582		
Family Watersiporidae						
Watersipora subtorquata	JN680947	NC_011820.2	NC_011820.2	AFK25576	YP_002456335	YP_002456339
Watersipora arcuata	FJ009090	AY789107		AAM46672		
Family Bitectiporidae						
Schizomavella linearis	JN680946	JN681077	JN681111	AEV21500	AEV21538	AEV21462
Pentapora foliacea	JN680941			AEV21497		AEV21458
Family Lanceoporidae						
*Calyptotheca immerse**	JF950374	JF950327		AEL29584		
Superfamily Schizoporelloidea						
Family Calwelliidae						
Calwellia gracilis	This study	This study	This study			This study
Family Margarettidae						
*Margaretta barbata**	JF950384	JF950306				
Family Buffonellodidae						
Aimulosia marsupium	This study					This study
Family Schizoporellidae						
Schizoporella dunkerii	JN680955		JN681118	AEV21509		AEV21470
Family Cryptosulidae						
Cryptosula pallasiana	JN680940	JN681073	JN681107	AEV21496		AEV21457
Family Margarettidae						
Margaretta barbata	JF950384	JF950306				
Family Escharinidae						
Phaeostachys sp	This study	This study		This study		
Hippomenella sp	This study	This study	This study			This study
*Hippomenella vellicata**	JF950403	JF950342		AEL29616		
Family Microporellidae						
Calloporina angustipora	JF950388	JF950321	EE	AEL29577	EE	EE
Fenestrulina littoralis AW423	EE	EE	EE		EE	EE
Fenestrulina specca AW436	EE	EE			EE	EE
Fenestrulina malusii LHL24	EE	EE	EE		EE	EE
Fenestrulina sp AW218	EE	EE			EE	
Fenestrulina sp LHL18	EE	EE	EE		EE	
Fenestrulina sp LHL28	EE	EE	EE			
Fenestrulina sp LHL30	EE	EE	EE		EE	
Fenestrulina thyrephora LHL40	EE				EE	EE

Tax. Level/Species	18S	16S	12S	cox1	cox3	cytb
Microporella sp AW520	EE			EE	EE	EE
Microporella speculum AW683	EE	EE	EE			EE
Microporella discors LHL5	EE	EE			EE	EE
Microporella diademata LHL11	EE		EE	EE	EE	EE
Microporella sp LHL15	EE				EE	EE
Microporella sp LHL25	EE	EE	EE		EE	EE
Microporella sp LHL27	EE	EE	EE		EE	
Microporella sp LHL29	EE		EE		EE	
Microporella intermediate LHL37			EE		EE	
Microporella ciliata LHL33	EE	AF156286		AEV21504		AEV21465
Microporella agonistes	JF950387	JF950343		AEL29613		
Superfamily Mamilloporoidea						
Family Cleidochasmatidae						
Cleidochasma cleidostoma	FJ009093	AY789094				
Family Crepidacanthidae						
*Crepidacantha crinispina**	JF950383	JF950326		AEL29597		
Crepidacantha zelanica	This study	This study				
Superfamily Celleporoidea						
Family Celleporoidae						
Celleporina hassallii	JN680945				AEV21537	AEV21461
Family Celleporidae						
Galeopsis sp.	This study	This study		This study	This study	This study
Family Phidoloporidae						
Reteporella beaniana	FJ196114			ACN91241		
*Phidoloporidae sp**		JN681084	JN681119	AEV21510	AEV21544	AEV21471
*Rhynchozoon zealandicum**	JF950380	JF950348		AEL29608		
Rhynchozoon	This study	This study		This study	This study	
Suborder Flustrina						
superfamily Catenicelloidea						
Family Catenicellidae						
Cribricellina cribraria	JF950401	JF950311				
Family Eurystomellidae						
*Eurystomella foraminigera**	JF950398	JF950304		AEL29605		
superfamily Cribrilinoidea						
Family Cribrilinidae						
Gephyrotes nitidopunctata	This study		This study			This study
Family Euthyroidae						
Euthyroides jellyae	JF950400	JF950309				
Superfamily Calloporoidea						
Family Foveolariidae						
Odontionella cyclops	This study		This study		This study	This study
Family Cupuladriidae						

Tax. Level/Species	18S	16S	12S	cox1	cox3	cytb
Cupuladria	This study		This study			This study
Family Akatoporidae						
Akatopora circumsaepta		This study	This study		This study	
Family Calloporidae						
Callopora lineata	JN680949	JN681080	JN681114	AEV21506	AEV21540	AEV21467
Family Chaperiidae						
*Chaperiopsis lanceola**	JF950397	JF950302		AEL29590		
*Chaperiopsis rubida**	JF950394	JF950332		AEL29600		
Superfamily Buguloidea						
Bugula fulva	FJ152023	JX183886		AFU49058		
Bugula turrita	AY210443	JX183889		AFZ78227		
Bugula plumosa	JN680951	JX183888		AFZ78225		
Bugula turbinata	FJ152024	KF714804		AHG98626		
*Bugula neritina**		KC130074		YP_001648398	AAT79553	AAT79560
Bugula stolonifera	AF499745	AY789087		AFZ78226		
Family Beaniidae						
Beania magellanica	JF950407	JF905315		AEL29589		
*Beania plurispinosa**	JF950408	JF950316		AEL29598		
Family Candidae						
Scrupocellaria scruposa	FJ196128			ACN91255		
Caberea rostrata	JF950396			AEL29581		
Superfamily Flustroidea						
Family Flustridae						
Flustra foliacea	FJ196110	NC_016722	NC_016722	YP_005089251.1	YP_005089248	YP_005089255
Superfamily Adeonoidea						
Family Adeonidae						
***Adeonellopsis*-like**	This study		This study			This study
Superfamily Microporoidea						
Family Otionellidae						
Otionellina sp.	This study	This study	This study		This study	
Family Cellarioidea						
Family Steginoporellidae						
Steginoporella magnifica	JF950369	JF950350		AEL29602		
Steginoporella sp	This study	This study	This study			This study
Family Microporoidea						
Micropora mortenseni	JF950371	JF950345		AEL29610		
Micropora sp	This study	This study	This study			
Opaeophora lepida	This study	This study	This study			
Suborder Malacostegina						
Superfamily Membraniporoidea						
Family Membraniporidae						
Membranipora membranacea	JN680943	JN681075	JN681109	AEV21498		AEV21459
Membranipora grandicella	AF499742			YP_006576069	YP_006576080	YP_006576081
Membranipora tuberculata	FJ009102	AY789095				
Family Electridae						

Tax. Level/Species	18S	16S	12S	cox1	cox3	cytb
Conopeum reticulum	JN680954	JN681083	JN681117		AEV21543	CCD33226
Conopeum seurati*	AM886860	KF714808		AHG98630		
Electra pilosa	JN680944	JN681076	JN681110	AEV21499	AEV21536	AEV21460
Electra arctica*	AM773515	AM773488				
Electra bellula	FJ009105	AY789088				
Electra scuticifera	FR754533	JF950340	FR754515	AEL29612		
Electra crustulenta	FR754535	AM773514	FR754518			
Electra korobokkura	AM158087	AJ853949	FR754516			
Electra posidonia	AM886850	AM747486	FR754514			
Electra verticillata*	FR754534	FR754524	FR754521			
Suborder Inovicellata						
Family Aeteidae						
Aetea anguina	JN680942	JN681074	JN681108		AEV21535	
Suborder Scrupariina						
Family Scrupariidae						
Scruparia chelata	JN680952	JN681081	JN681115	AEV21507	AEV21541	AEV21468
Family Eucrateidae						
Eucratea loricata	AM886856	AM747489				

Appendix 2: Materials and methods

Primer combinations	Size	gene	Cycling profile Dreamtaq				
			40 cycles				
Bryozoa_12SF + Bryozoa_12SR	586	12S	94 °C 3 m	94 °C 30 s	48 °C 30 s	72 °C 1 m	72 °C 10 m
Cheilo_12SF_seq + Cheilo_12SR_seq	290	12S			48 °C 30 s		
Bryozoa_16SF + Bryozoa_16SR	927	16S			43 °C 30 s		
cox1F_prifi + cox1R_prifi	620	Cox1			53 °C 30 s		
cox1F_prifi + cox1R_prifi_M13F(-20)	620	Cox1			62 °C 30 s		
Bryozoa_cox3F + Bryozoa_cox3R_M13F(-20)	589	Cox3			55 °C 30 s		
Bryozoa_cytbF_B + Bryozoa_cytbR	422	Cytb			48 °C 30 s		
18e + Gymno300R	209	18S	94 °C 3 m	94 °C 30 s	54 °C 30 s	72 °C 2 m	72 °C 10 m
Gymno300F + 18p	1630	18S			54 °C 30 s		
Gymno300F + Gymno1200R	1264	18S			54 °C 30 s		
			Cycling profile Phusion high-fidelity				
			35 cycles				
Bryozoa_12SF + Bryozoa_12SR	586	12S	94 °C 30 s	94 °C 30 s	58.5 °C 30 s	68 °C 1 m	68 °C 5 m
Cheilo_12SF_seq + Cheilo_12SR_seq	290	12S			58.5 °C 30 s		
Cheilo12S627_F + Cheilo12s257_R	370	12S			47 °C 30 s		
Bryozoa_16SF + Bryozoa_16SR	927	16S			47 °C 30 s		
cox1F_prifi + cox1R_prifi	620	Cox1			51.5 °C 30 s		
cox1F_prifi + cox1R_prifi_M13F(-20)	620	Cox1			58 °C 30 s		
F2bryCOI + R2bryCOI		Cox1			54 °C 30 s		
Bryozoa_cox3F + Bryozoa_cox3R_M13F(-20)	589	Cox3			55 °C 30 s		
Bryozoa_cytbF_B + Bryozoa_cytbR	422	Cytb			47 °C 30 s		
18e + Gymno300R	209	18S	94 °C 30 s	94 °C 30 s	58.5 °C 30 s	68 °C 2 m	68 °C 5 m
Gymno300F + 18p	1630	18S			58.5 °C 30 s		
Gymno300F + Gymno1200R	1264	18S			58.5 °C 30 s		
Cheilo18S156_F + Cheilo18s1660_R	1540	18S			57 °C 30 s		

Table A2.1: PCR primer combinations and cycling profiles for both polymerase types used in this study. Size: predicted size of amplicon in nucleotides.
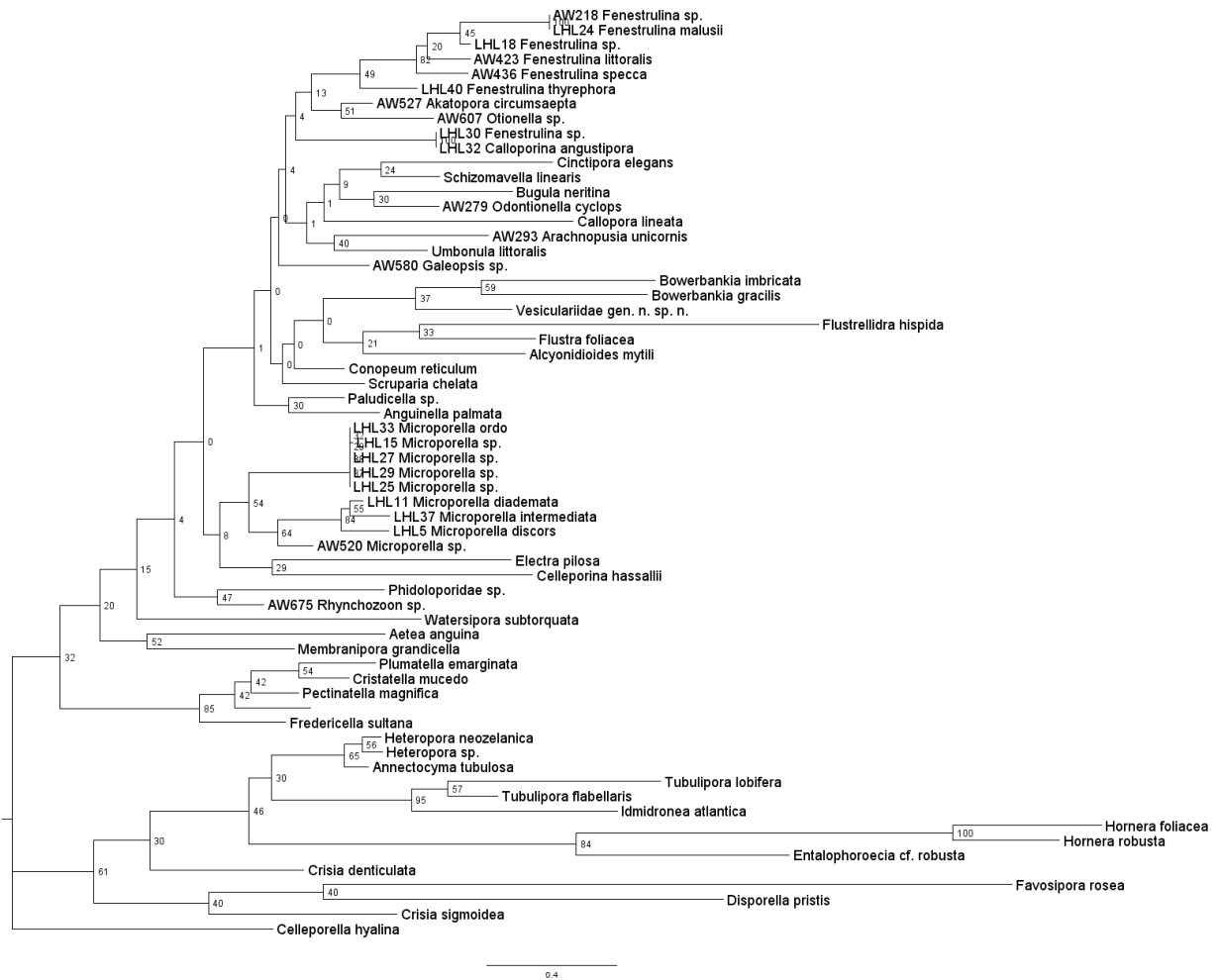
Figure A2.1: Phylogenetic ML inference of 18S sequences. Tree inference done in RAxML based on a dataset with 165 taxa and 1390 nucleotide positions. 100 topology searches and 100 boostrap searches using the GTR+i+g model of evolution.

46
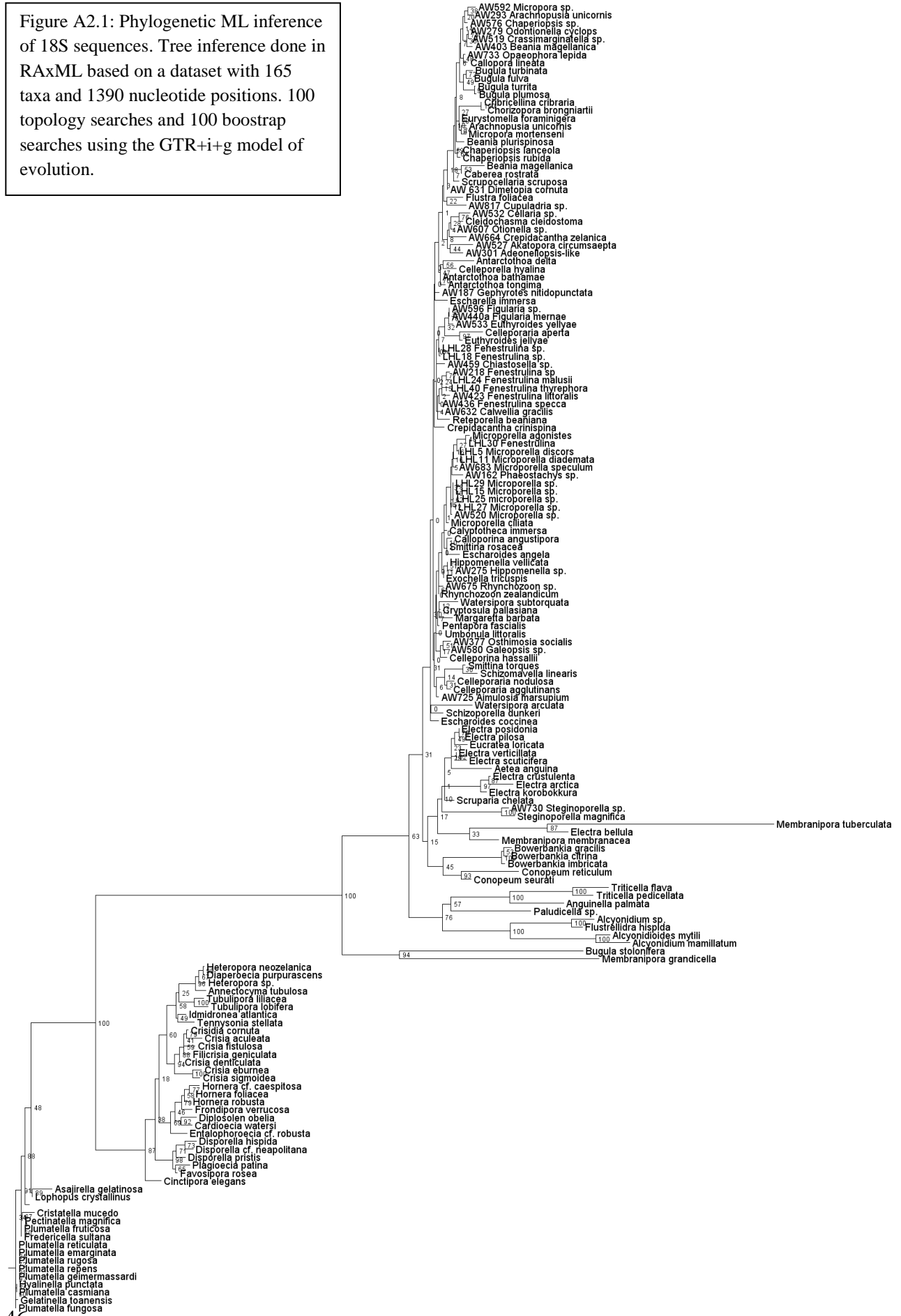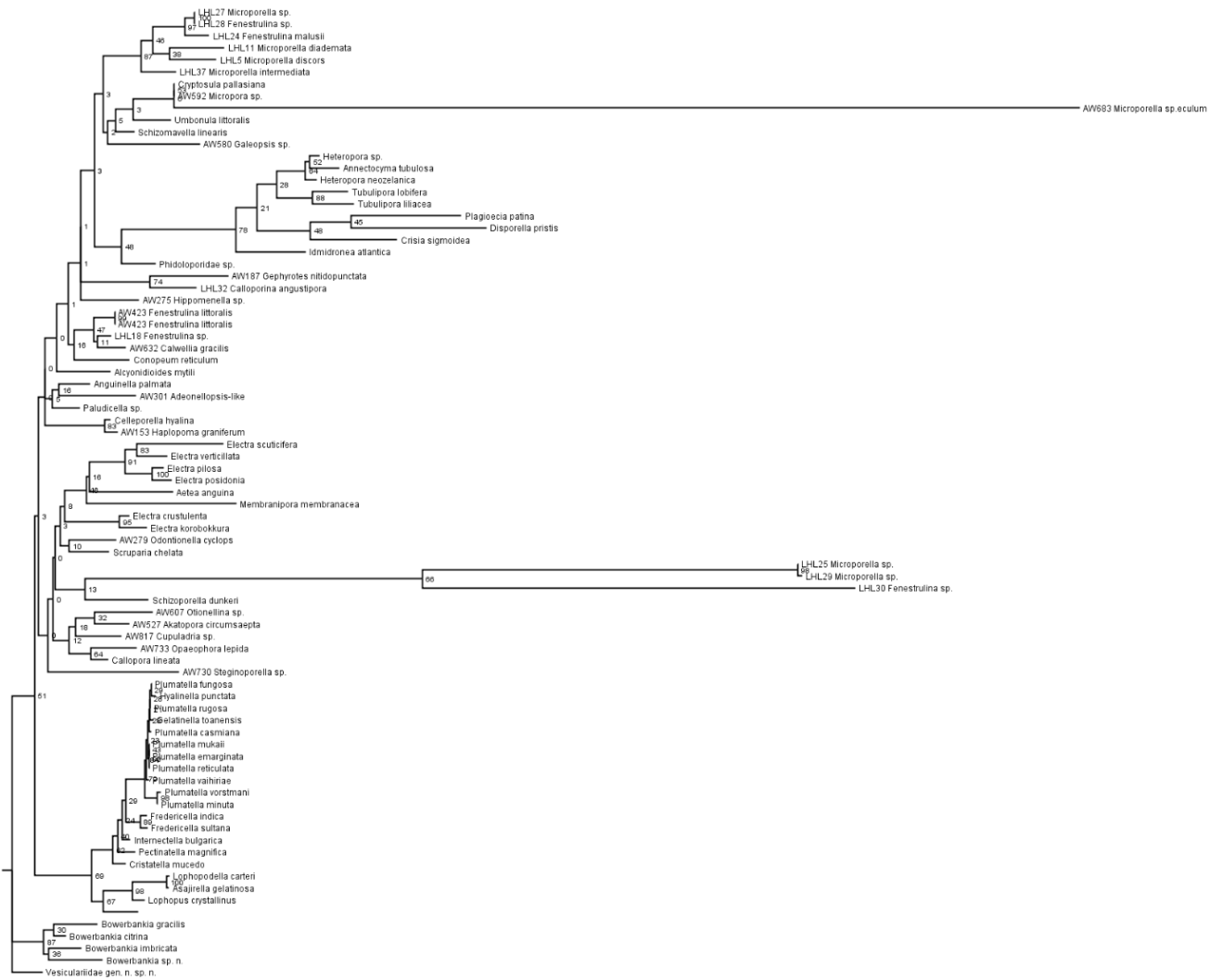
Figure A2.2: Phylogenetic ML inference of 12S sequences. Tree inference done in RAxML based on a dataset with 81 taxa and 339 nucleotide positions. 100 topology searches and 100 bootstrap searches using the GTR+i+g model of evolution.

Figure A2.3: Phylogenetic ML inference of 16S sequences. Tree inference done in RAxML based on a dataset with 129 taxa and 336 nucleotide positions. 100 topology searches and 100 bootstrap searches using the GTR+i+g model of evolution.
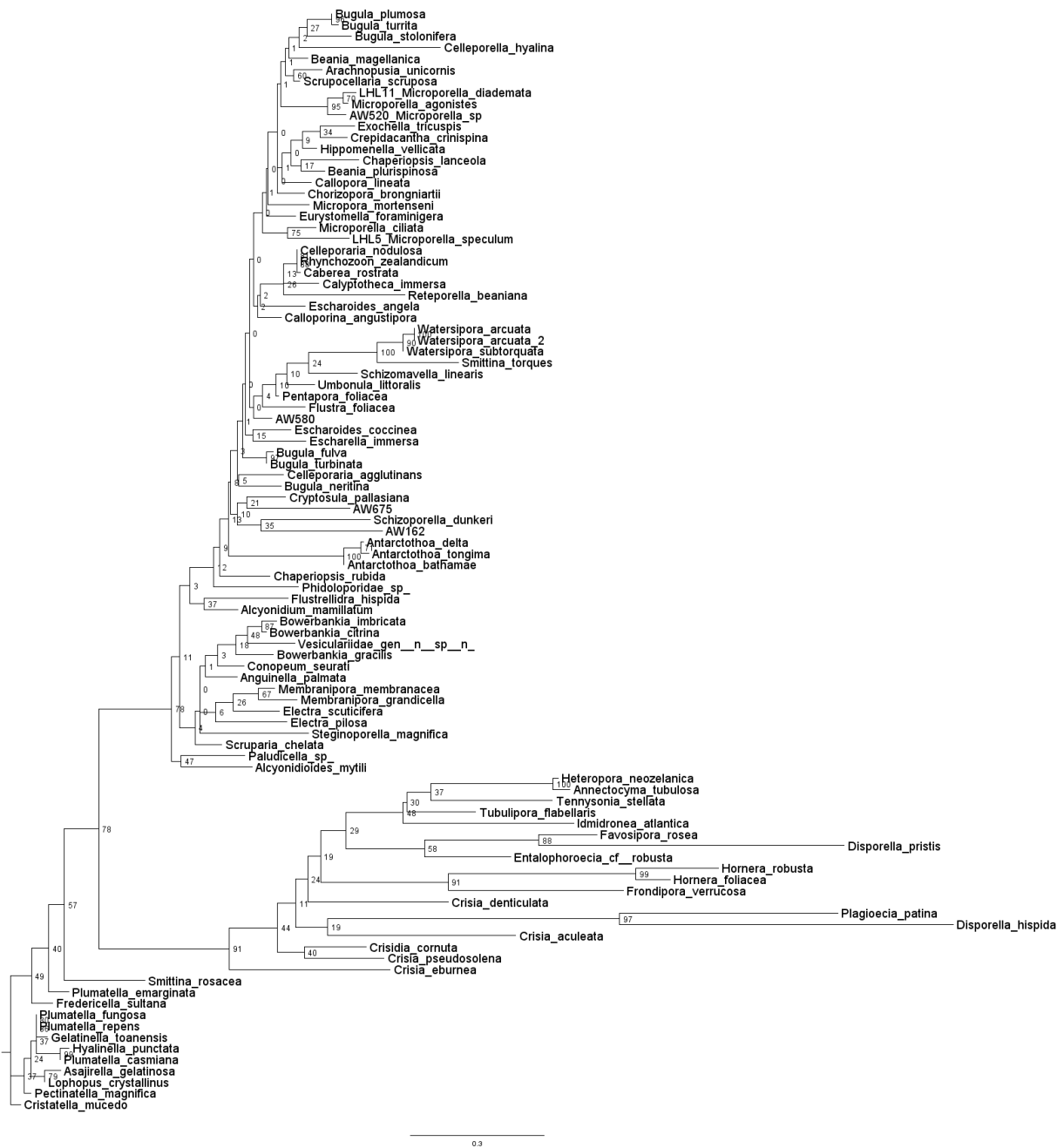
Figure A2.4: Phylogenetic ML inference of Cox1 sequences. Tree inference done in RAxML based on a dataset with 99 taxa and 408 amino acid positions. 100 topology searches and 100 bootstrap searches using the rtREV +i+g model of evolution.

Figure A2.5: Phylogenetic ML inference of Cox3 sequences. Tree inference done in RAxML based on a dataset with 63 taxa and 173 amino acid positions. 100 topology searches and 100 bootstrap searches using the rtREV+i+g model of evolution.

Figure A2.6: Phylogenetic ML inference of CytB sequences. Tree inference done in RAxML based on a dataset with 82 taxa and 130 amino acid positions. 100 topology searches and 100 boostrap searches using the rtREV+i+g model of evolution.

Appendix 3: Results

	lambda0	lambda1	mu0	mu1	q01	q10
(1) Full model	21.018643	30.63602	16.97583	12.54635	0.1475167	2.9429999
(2) Equal speciation	NA	31.04348	26.84736	14.44566	0.1783575	0.4187066
(3) Equal extinction	20.086652	33.29166	15.95024	NA	0.1682257	2.8019589
(4) Equal transition	27.398328	38.47800	22.85842	23.67199	0.2687969	NA
(5) No extinction	6.3565146	21.7936188	NA	NA	0.2236949	4.0457489
(6) No q10	25.3727148	40.1687035	20.2482138	24.5798138	0.3957528	NA
(7) No ext. no q10	8.401506	22.00125	NA	NA	0.4287095	NA

Table A3.1: BiSSE estimated parameter values for the different models. First column: models as in described in the methods.

lambda1	lambda1	lambda1	lambda1	lambda1
1.193212e+01	2.130591e+01	2.934725e+01	2.690204e+01	8.970189e+00
lambda1	**lambda1**	**lambda1**	**lambda1**	**q**
1.322500e-07	1.438404e-08	1.959251e+01	4.971703e+00	1.346161e-01
df	**lnLik**	**AIC**		
10	3.230587	13.53883		

Table A3.2: Estimated parameters based on a MuSSE model with all transition states equal, and all extinction rates 0. Result of running a Maximum Likelihood Estimation of the model.

Figure A3.1: Phylogenetic ML inference of Dataset Two. Tree inference done in RAxML based on a dataset with 111 taxa, 2155 nucleotides and 713 amino acid positions. 100 topology searches and 500 boostrap searches have been run using the GTR+i+g model of evolution for the nucleotide partition and rtREV+i+g model of evolution for the amino acid partition.
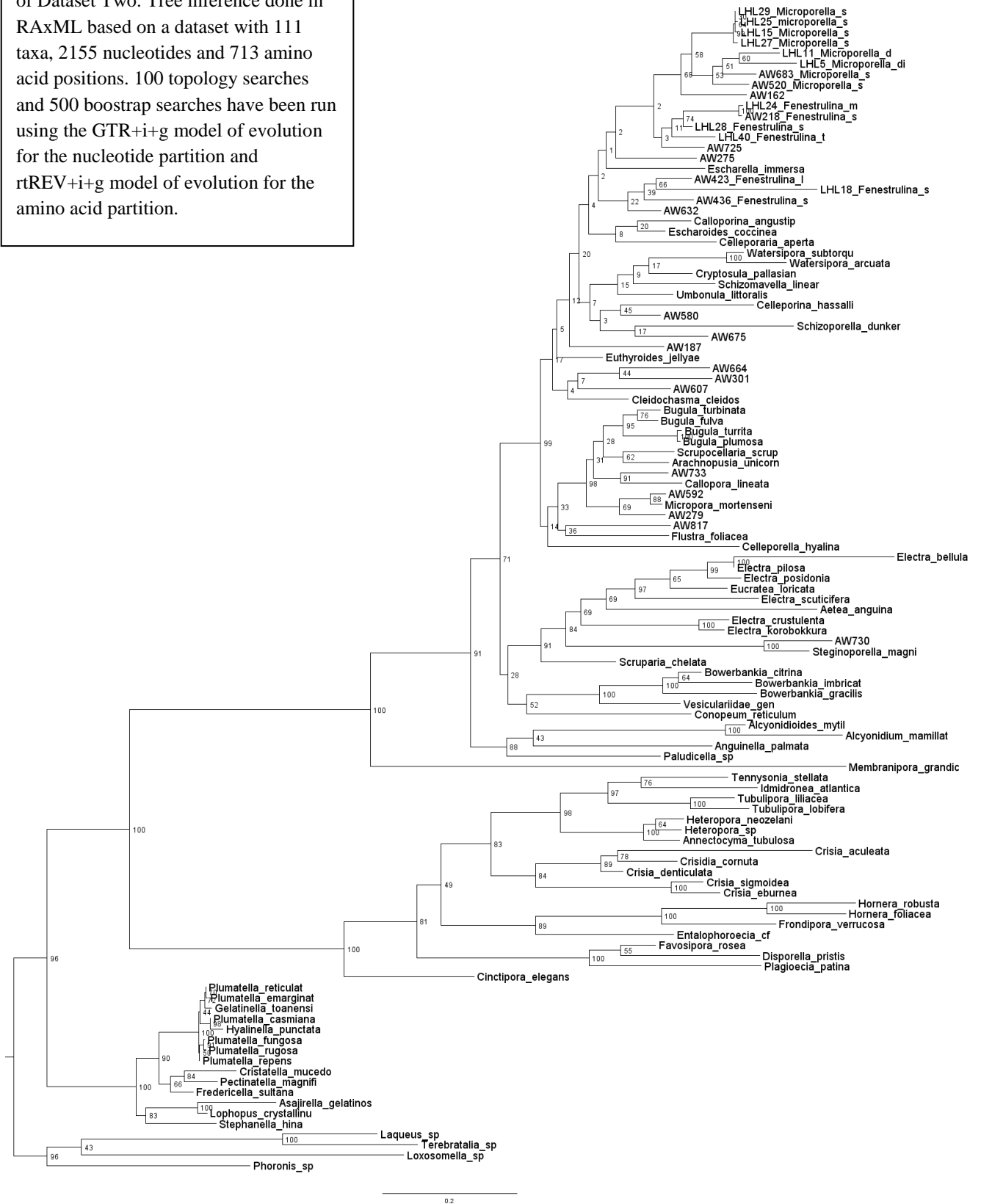
Figure A3.2: Phylogenetic ML inference of Dataset One. Tree inference done in RAxML based on a dataset with 134 taxa, 2155 nucleotides and 713 amino acid positions. 100 topology searches and 500 boostrap searches have been run using the GTR+i+g model of evolution for the nucleotide partition and rtREV+i+g model of evolution for the amino acid partition.

Outgroup

60.0

600   500   400   300   200   100   0
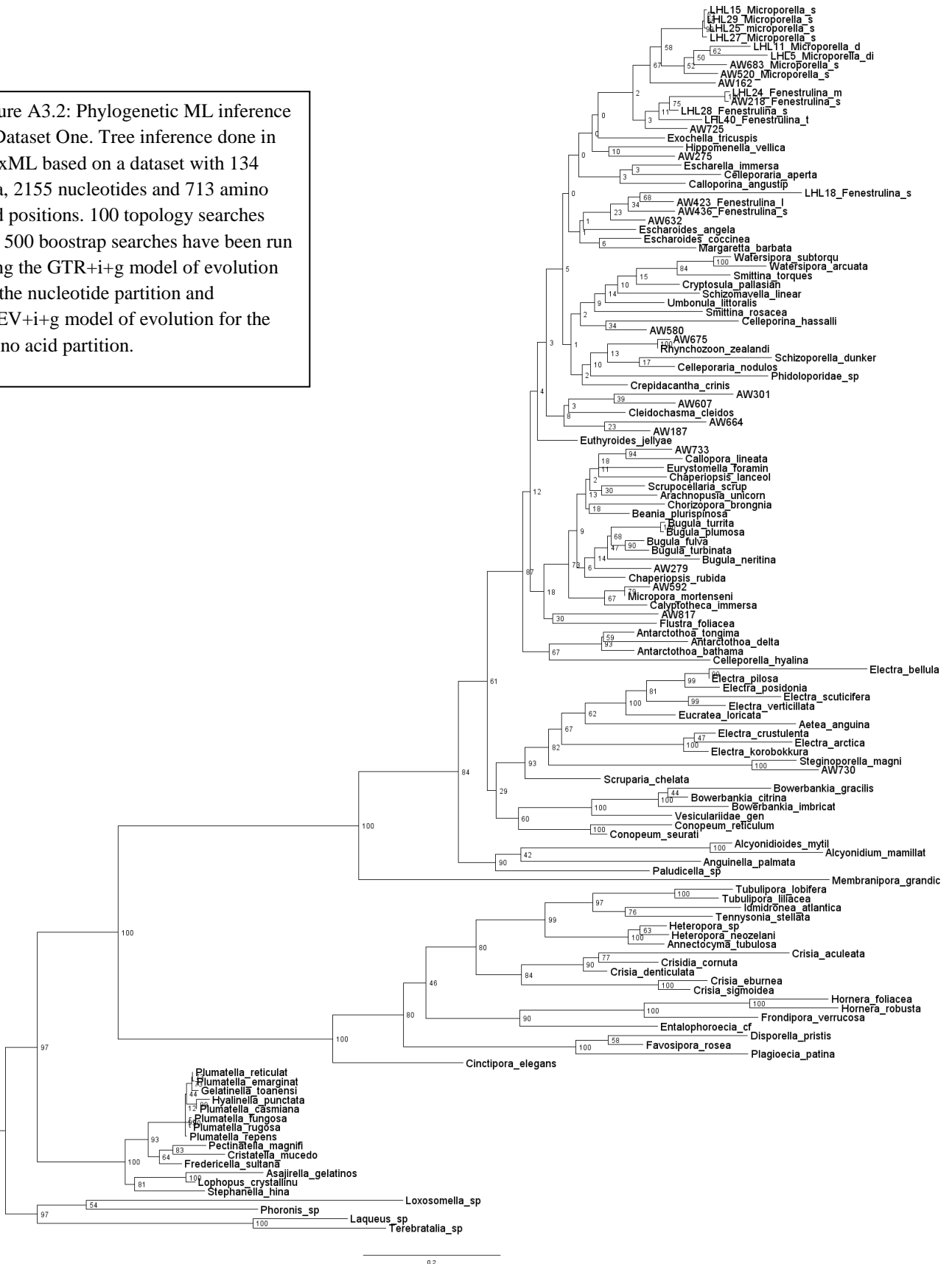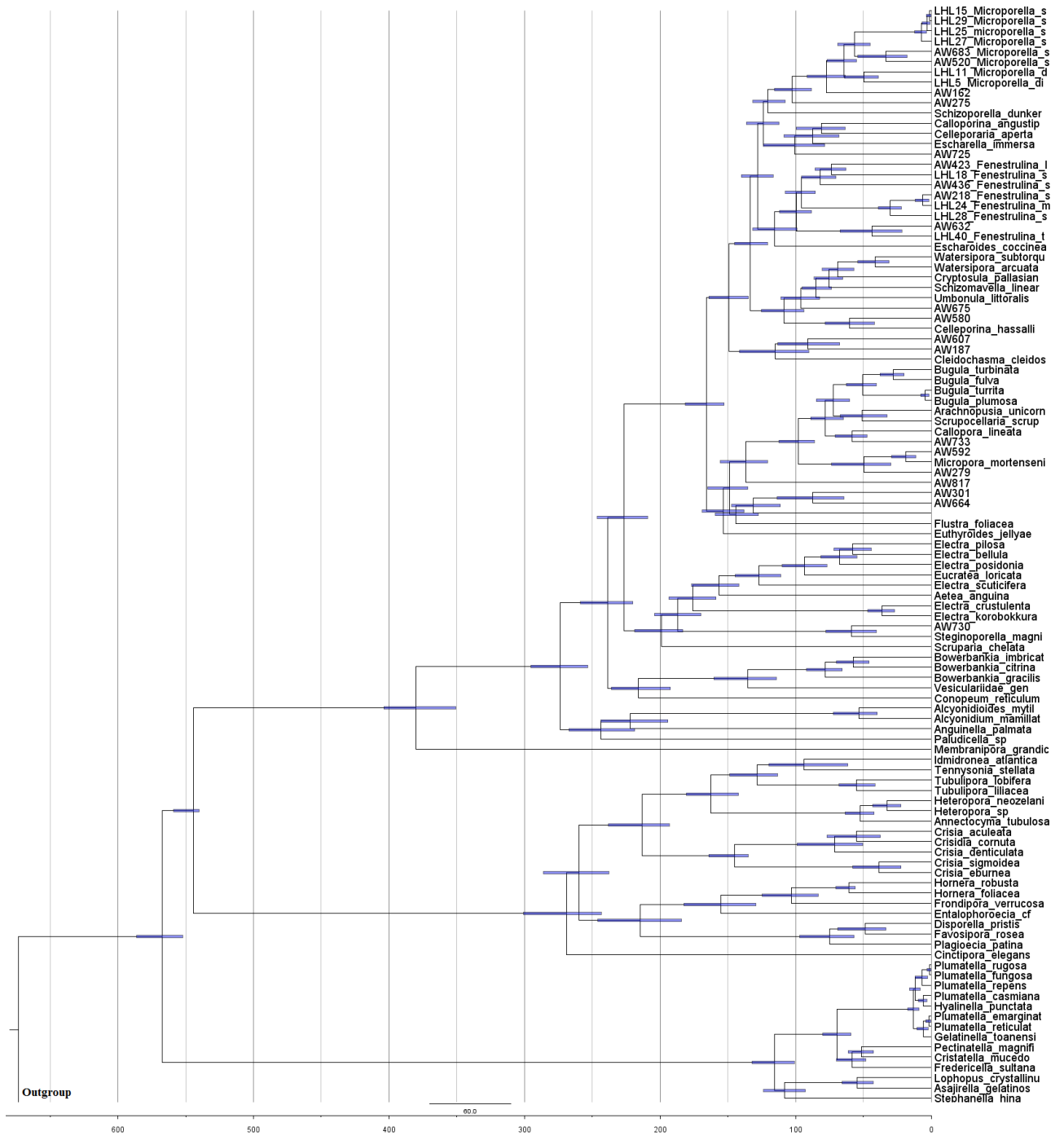
Figure A3.3: Fossil calibrated phylogeny, produced with FDPPDiv running under a strict clock. 6.000 out of 100.000 generations discarded as burn-in Scale bar represent time in millions of years. Blue node bars represent 95% highest density probabilities based off the Bayesian inference.

55

Appendix 4: Newly sequenced species

Calwellia gracilis, **Maplestone, 1882**

Family Calwelliidae

Frontal wall: lepraliomorph

Specimen ID: AW632
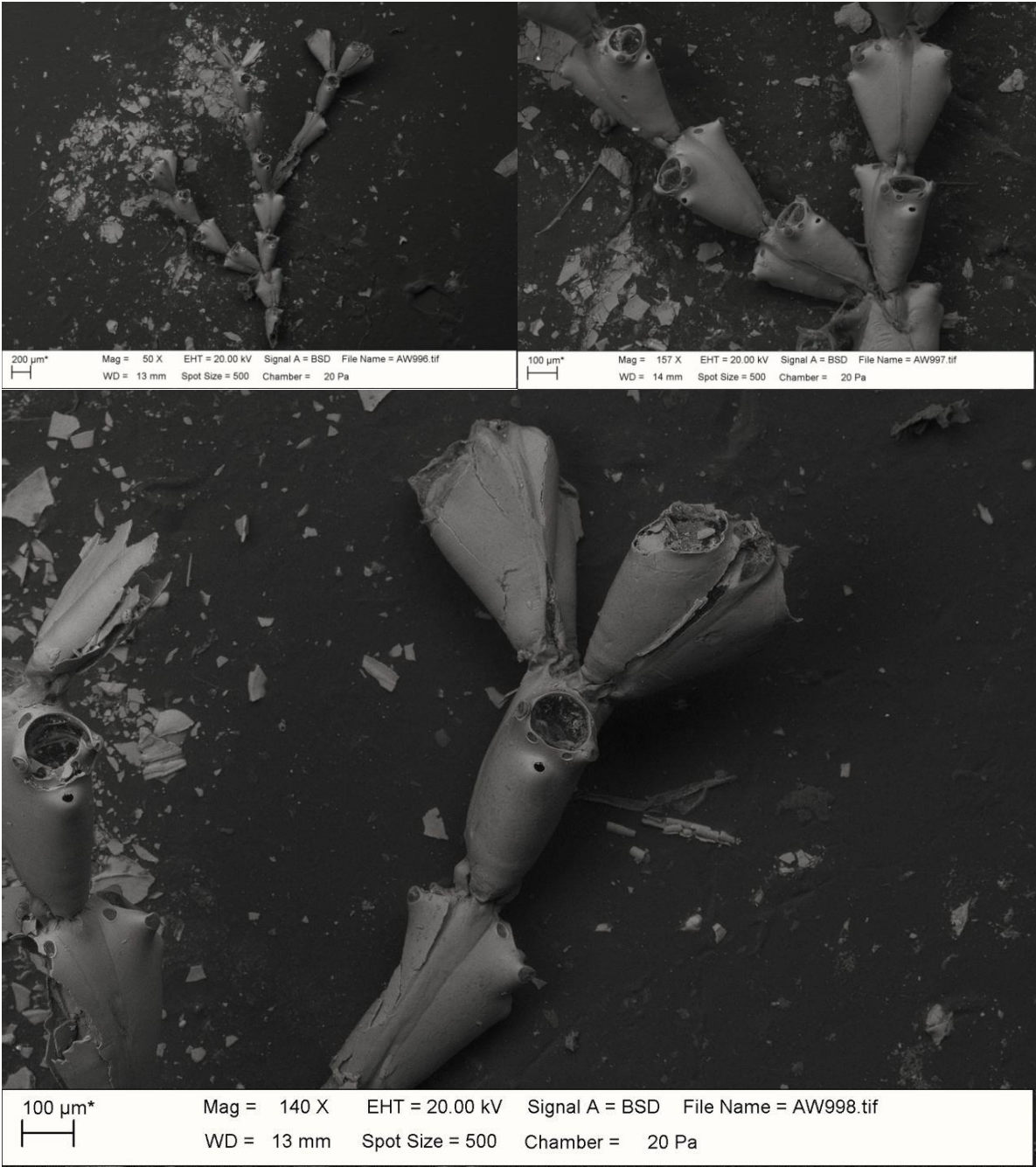
Pictures credit: Andrea Waeschenbach, NHMUK.

Aimulosia marsupium, **MacGillivray, 1869**

Family Buffonellodidae

Frontal wall: lepraliomorph

Specimen ID: AW725
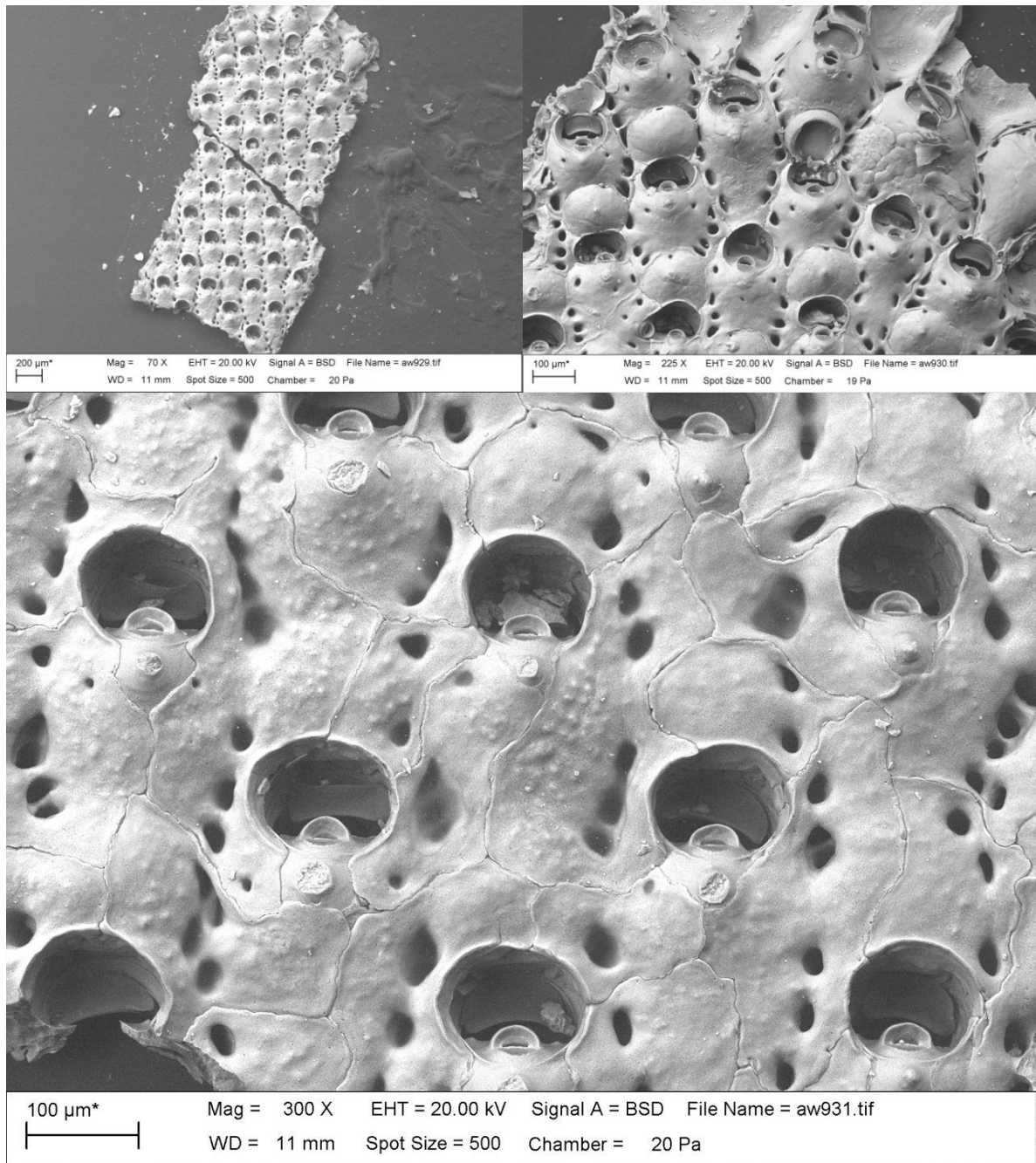
Pictures credit: Andrea Waeschenbach, NHMUK.

Phaeostachys sp. **Hayward, 1979**

Family Escharinidae

Frontal wall: lepraliomorph

Specimen ID: AW162
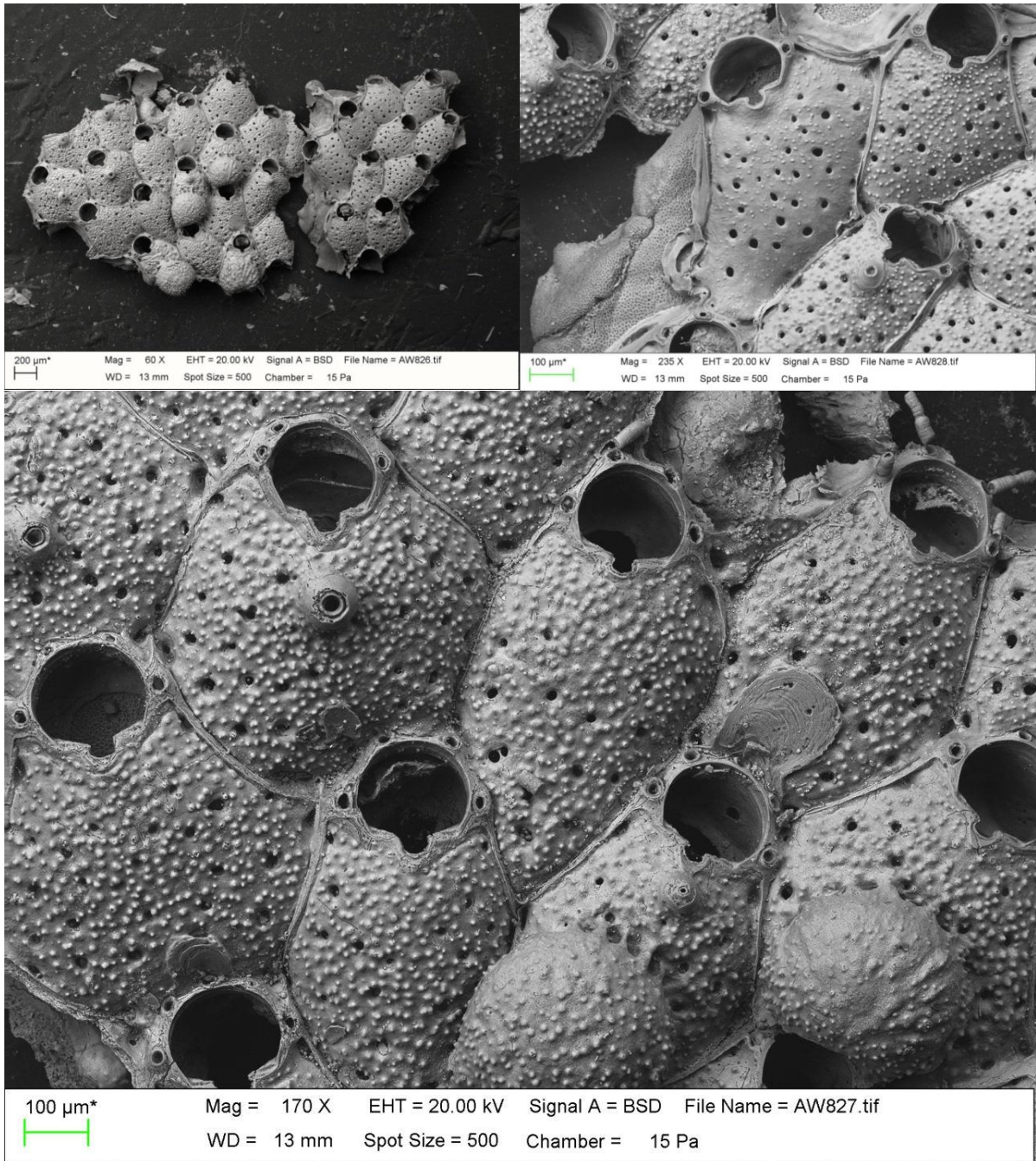
Pictures credit: Andrea Waeschenbach, NHMUK.

Hippomenella sp, **Canu & Bassler, 1917**

Family Escharinidae

Frontal wall: lepraliomorph

Specimen ID: AW275
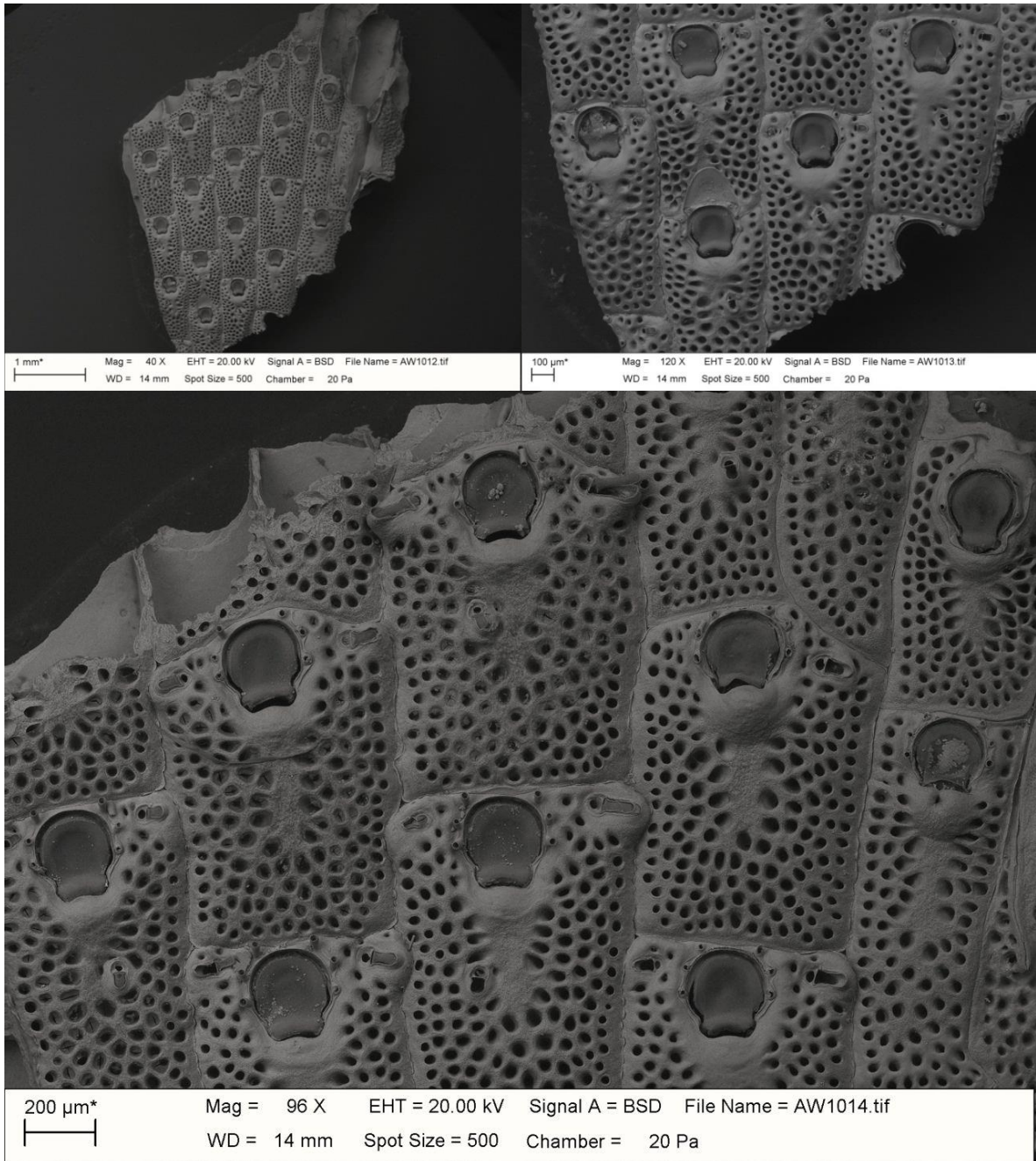
Pictures credit: Andrea Waeschenbach, NHMUK.

Crepidacantha zelanica, **Canu & Bassler, 1929**

Family Crepidacanthidae

Frontal wall: lepraliomorph

Specimen ID: AW664
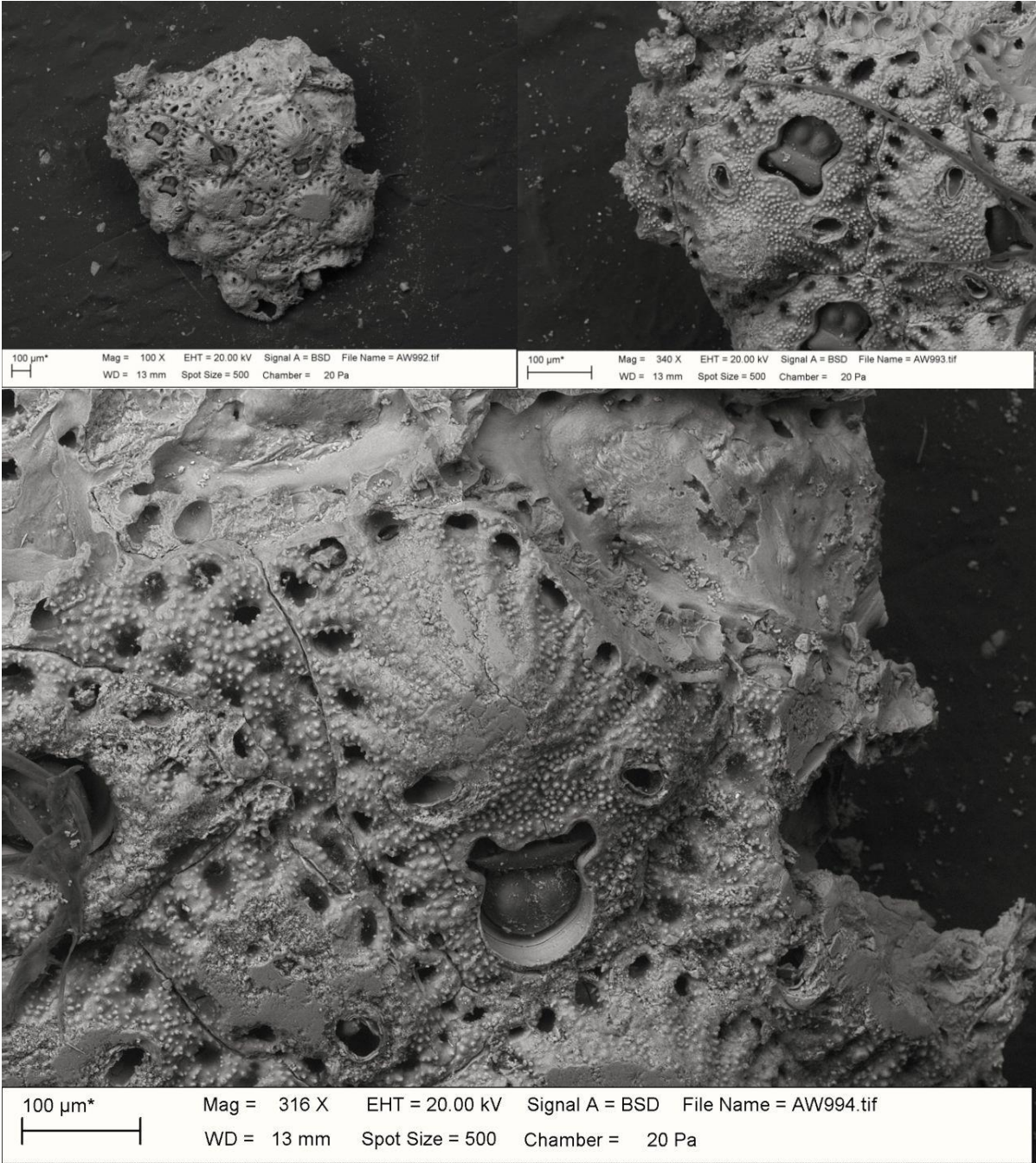
Pictures credit: Andrea Waeschenbach, NHMUK.

Galeopsis sp. **Jullien, 1903**

Family Celleporidae

Frontal wall: lepraliomorph

Specimen ID: AW580
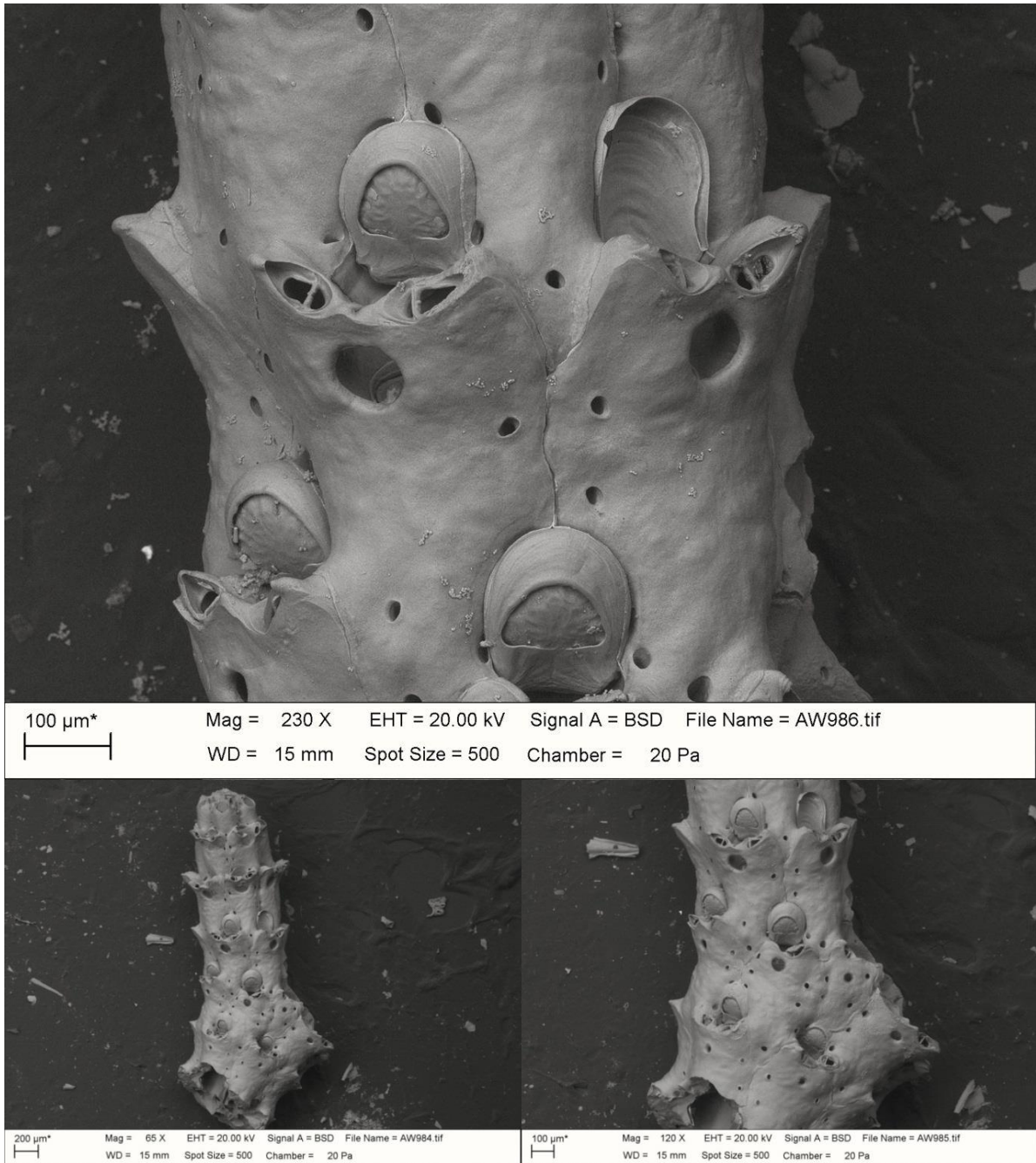
Pictures credit: Andrea Waeschenbach, NHMUK.

Rhynchozoon sp. **Hincks, 1895**

Family Phidoloporidae

Frontal wall: lepraliomorpha

Specimen ID: AW675
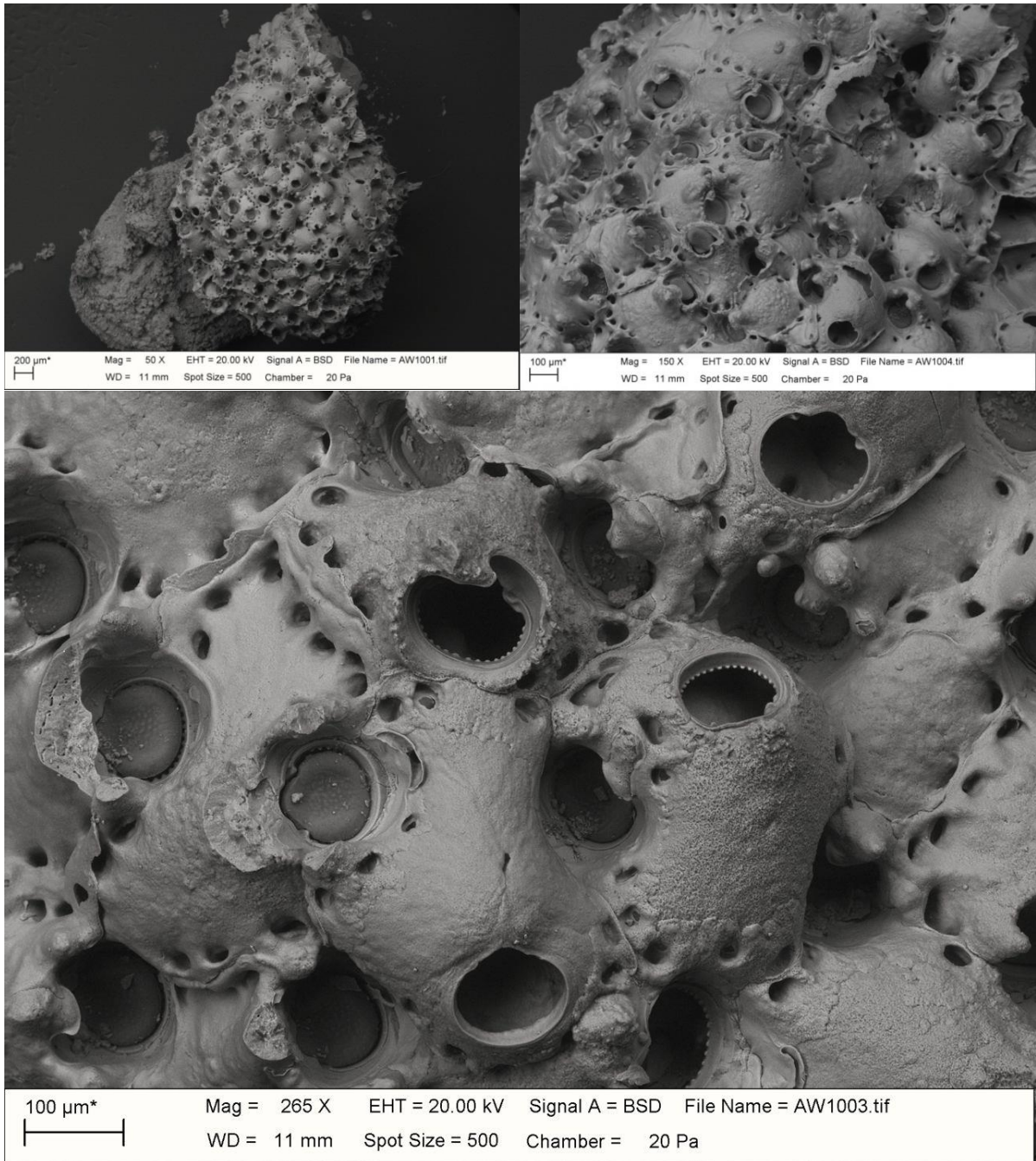
Pictures credit: Andrea Waeschenbach, NHMUK.

Gephyrotes nitidopunctata, **Smitt, 1868**

Family Cribrilinidae

Frontal wall: acanthostega

Specimen ID: AW187
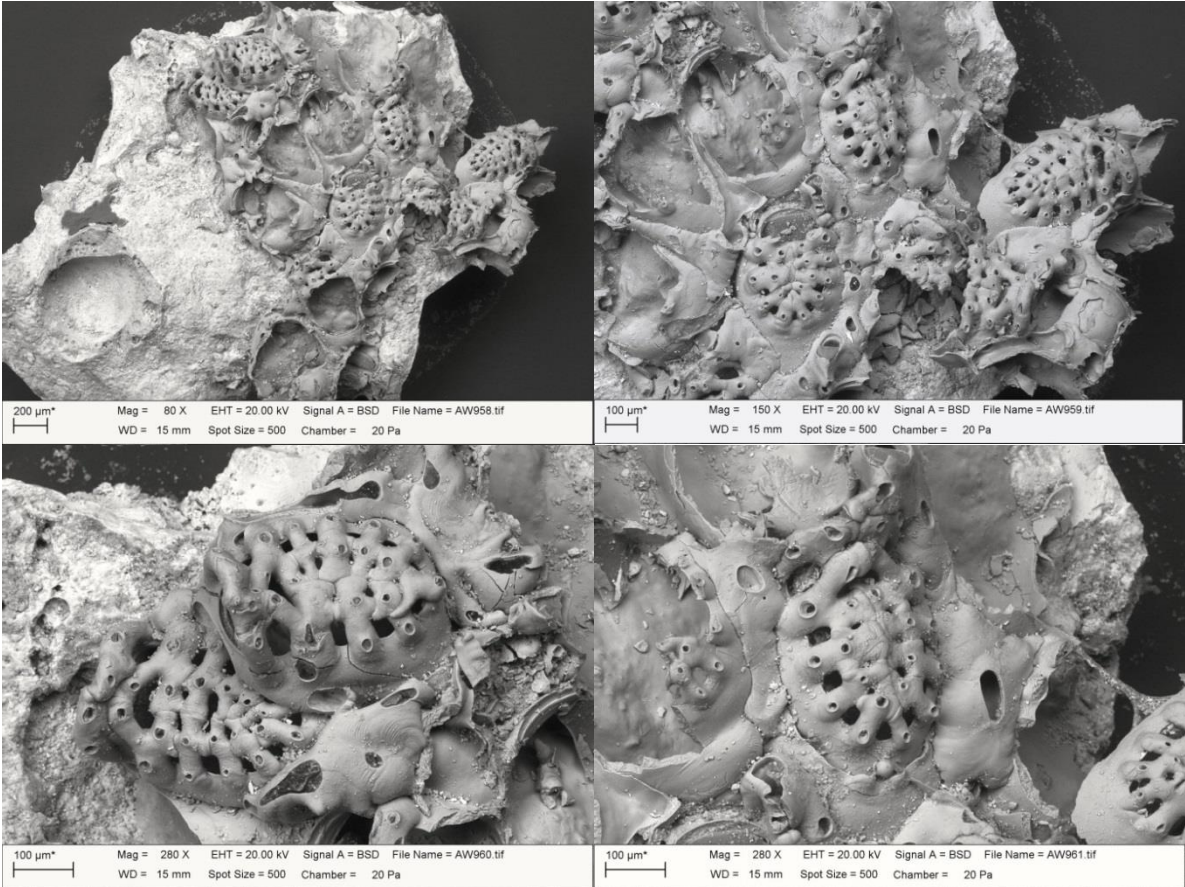
Pictures credit: Andrea Waeschenbach, NHMUK.

Odontionella cyclops, **Busk, 1854**

Family Foveolariidae

Frontal wall: flustrina

Specimen ID: AW279
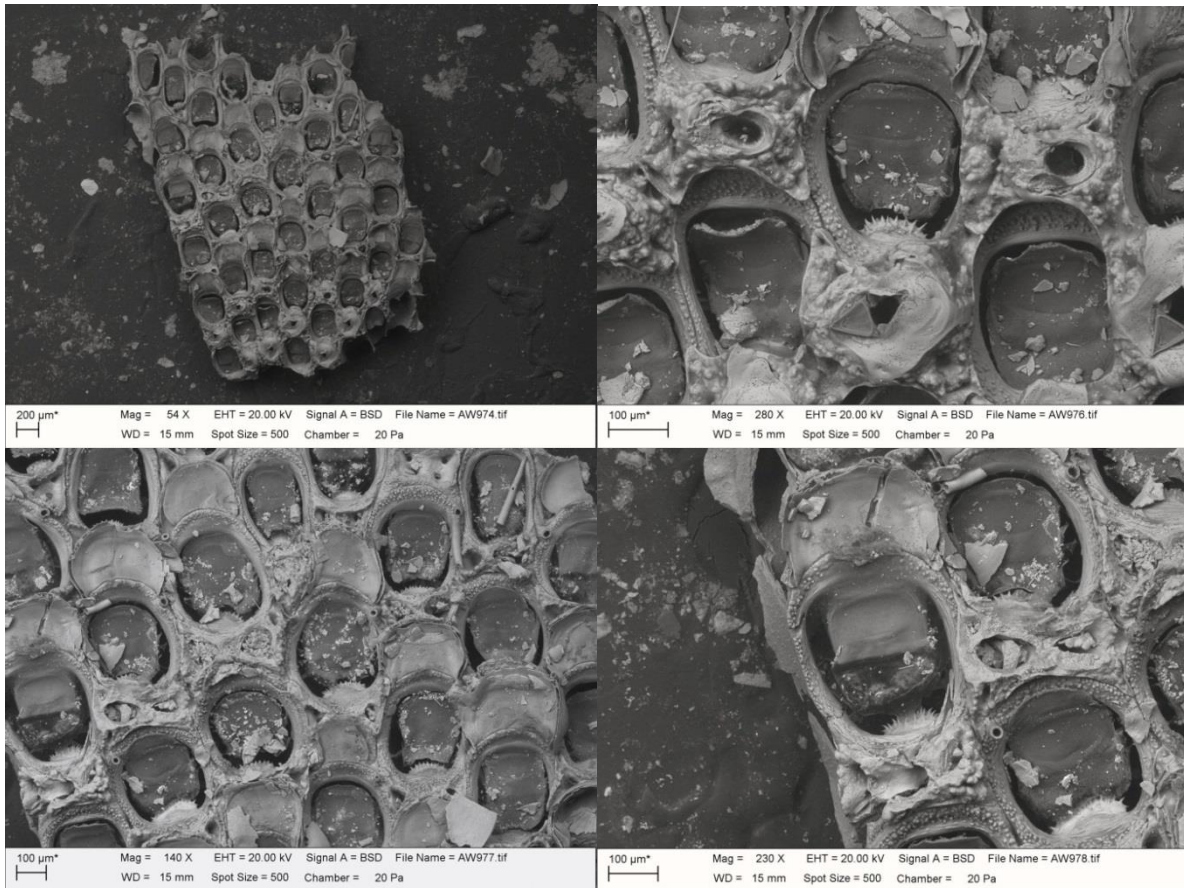
Pictures credit: Andrea Waeschenbach, NHMUK.

Cupuladria sp. **Canu & Bassler, 1919**

Family Cupuladriidae

Frontal wall: flustrina

Specimen ID: AW817
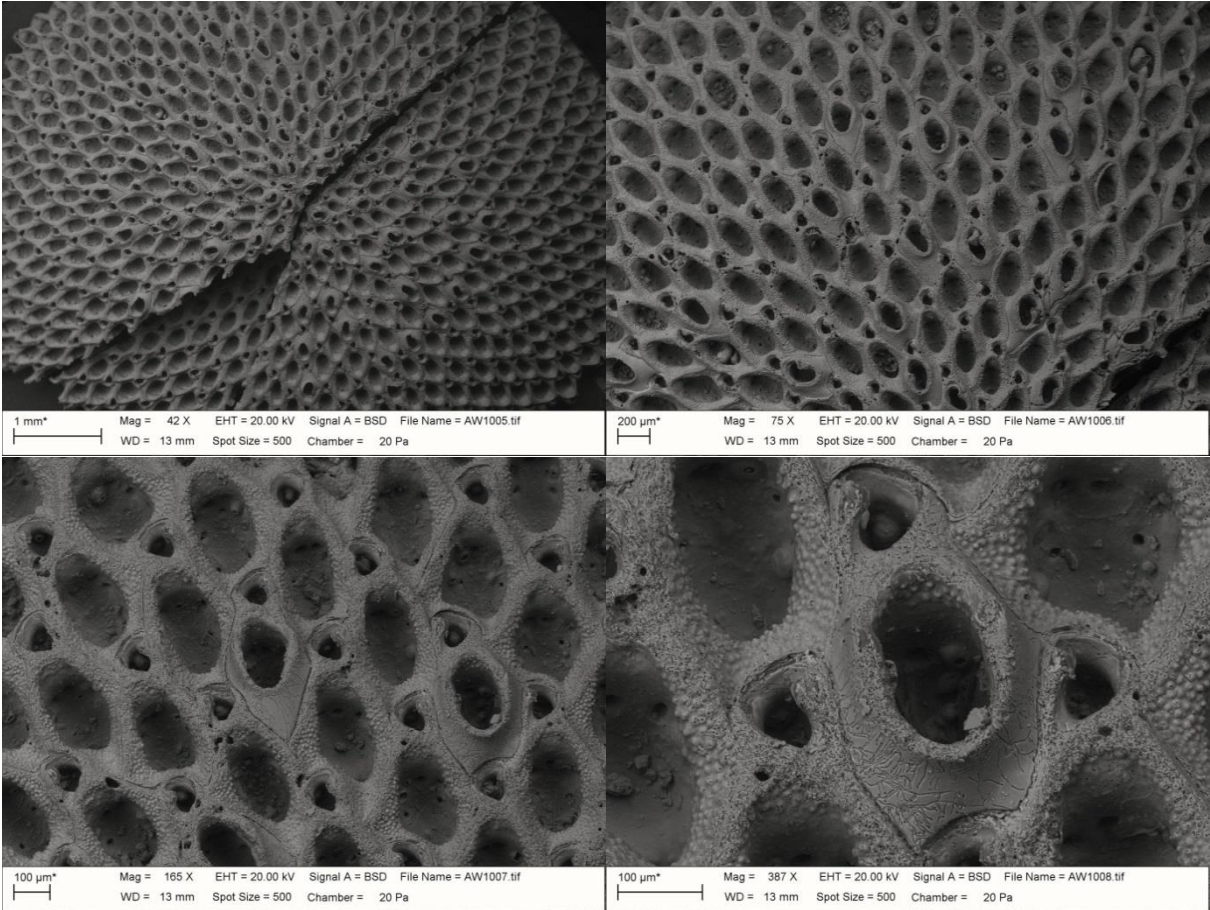
Pictures credit: Andrea Waeschenbach, NHMUK.

Akatopora circumsaepta, **Uttley, 1951**

Family Akatoporidae

Frontal wall: flustrina

Specimen ID: AW527
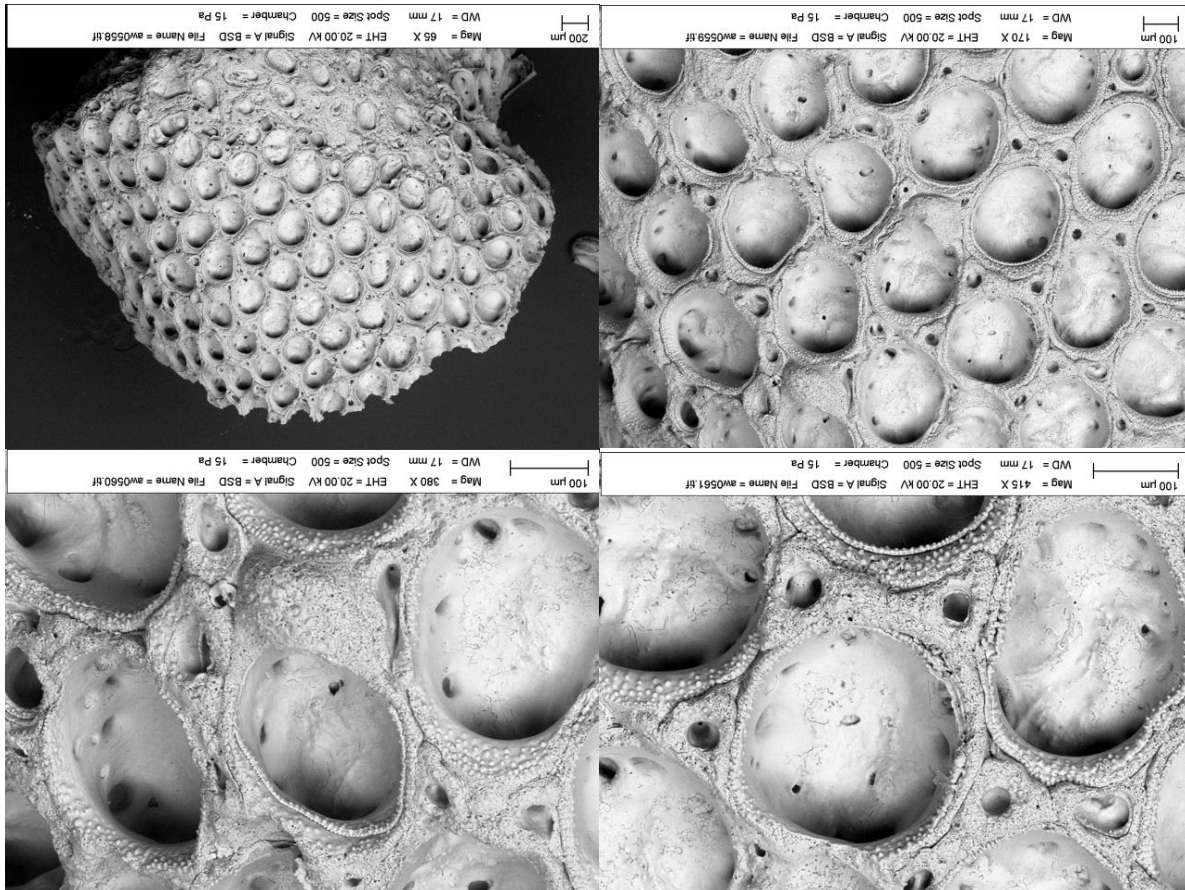
Pictures credit: Andrea Waeschenbach, NHMUK.

Adeonellopsis (?) (*Adeonellopsis sp.* **MacGillivray, 1886)**

Family Adeonidae

Frontal wall: umbomulomorpha

Specimen ID: AW301
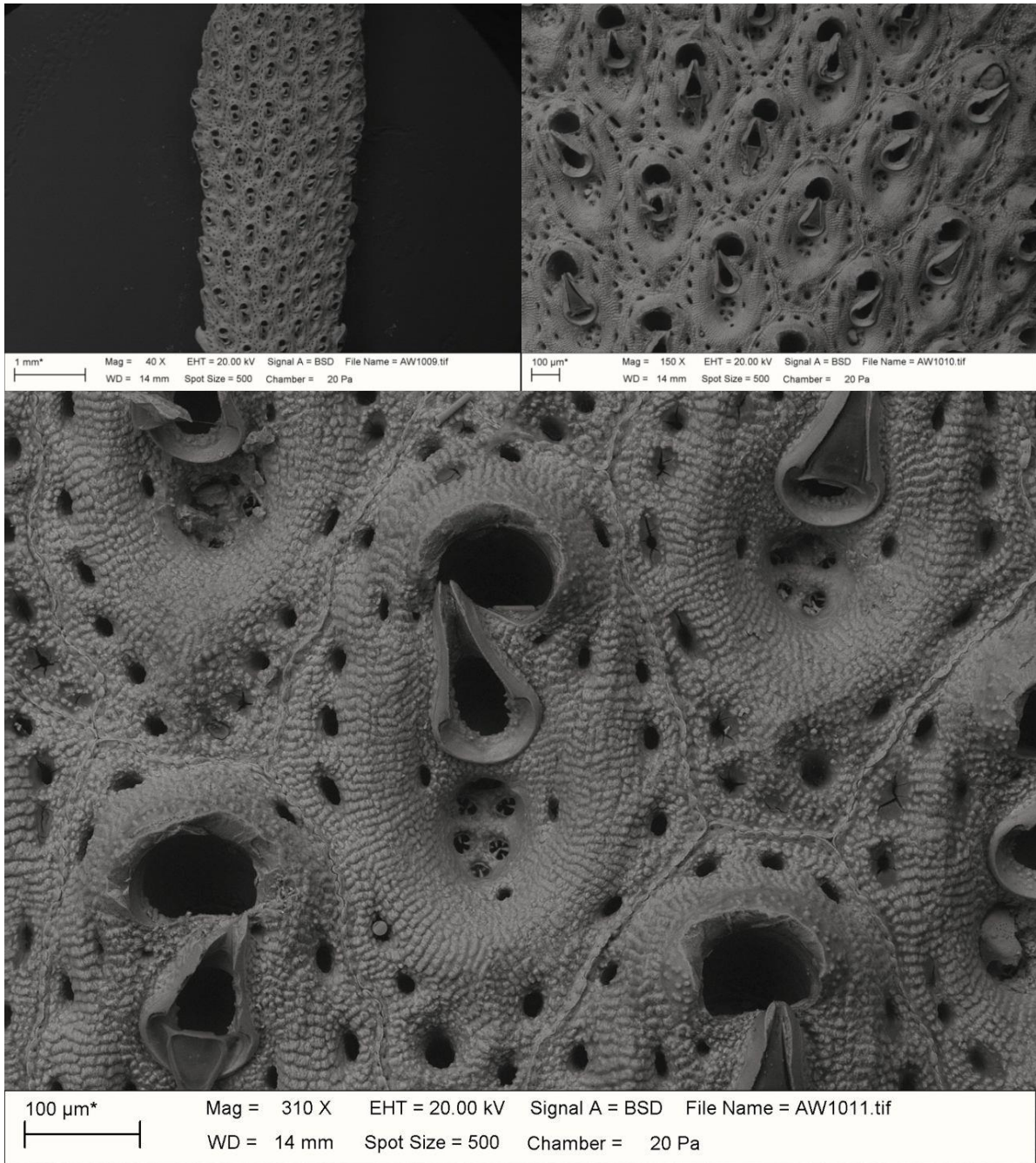
Pictures credit: Andrea Waeschenbach, NHMUK.

Otionellina sp. **Bock & Cook, 1998**
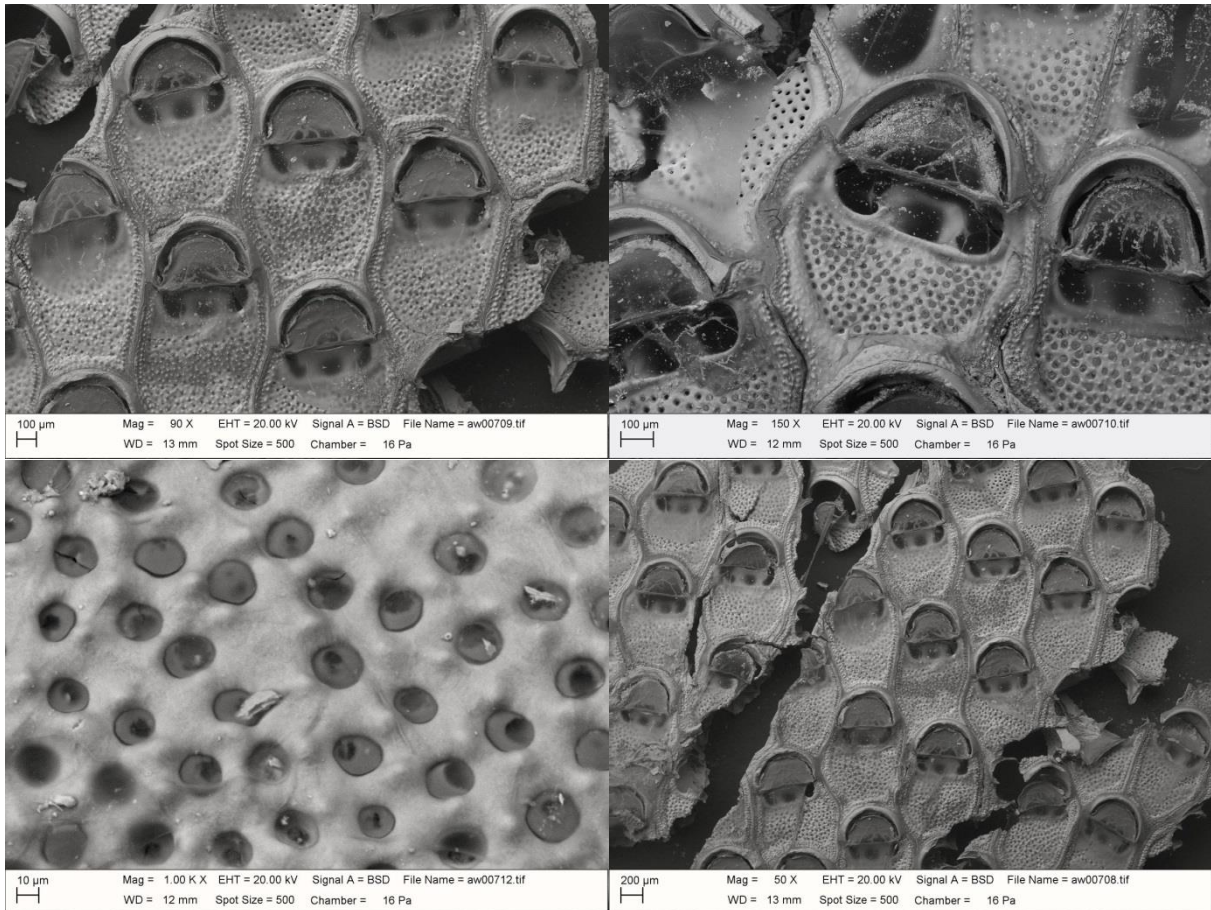
Family Otionellidae

Frontal wall: flustrina

Specimen ID: AW607
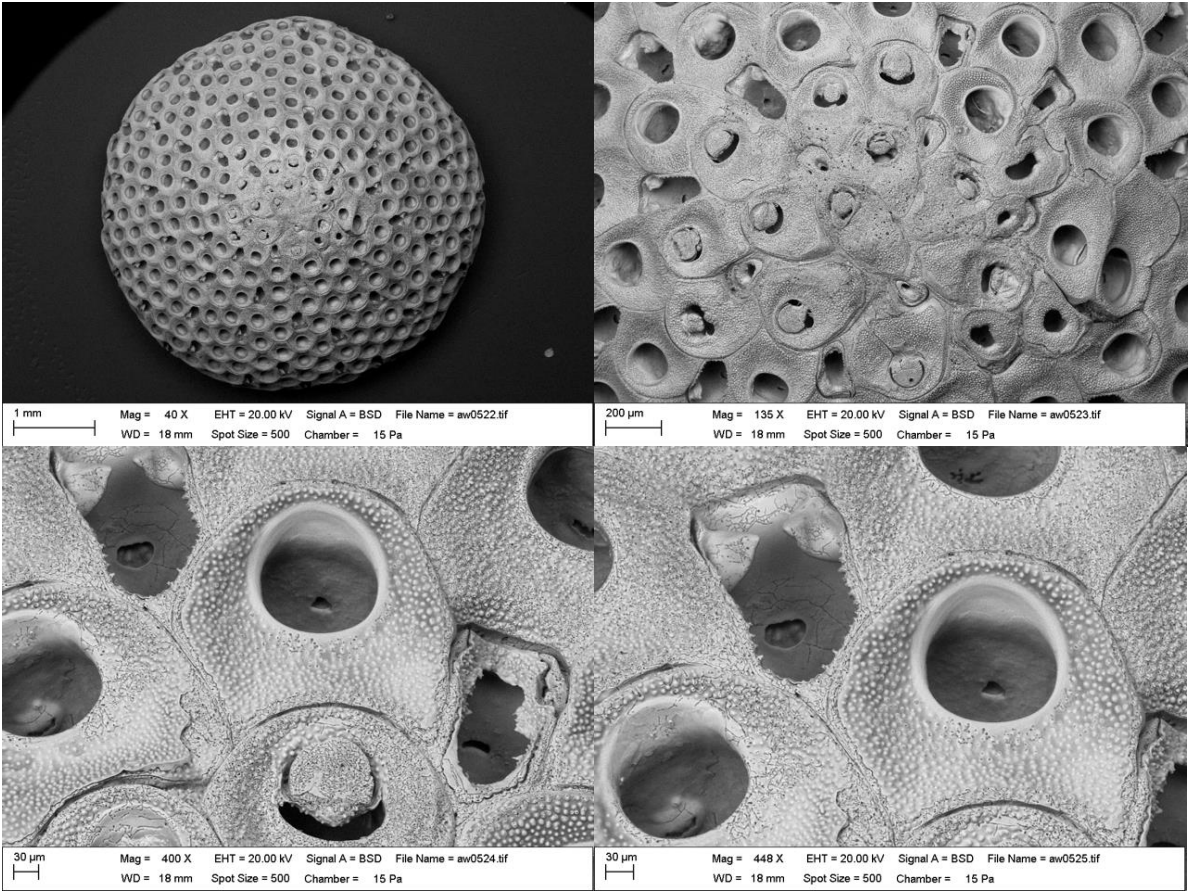
Pictures credit: Andrea Waeschenbach, NHMUK.

Steginoporella sp. **Smitt, 1873**

Family Steginoporellidae

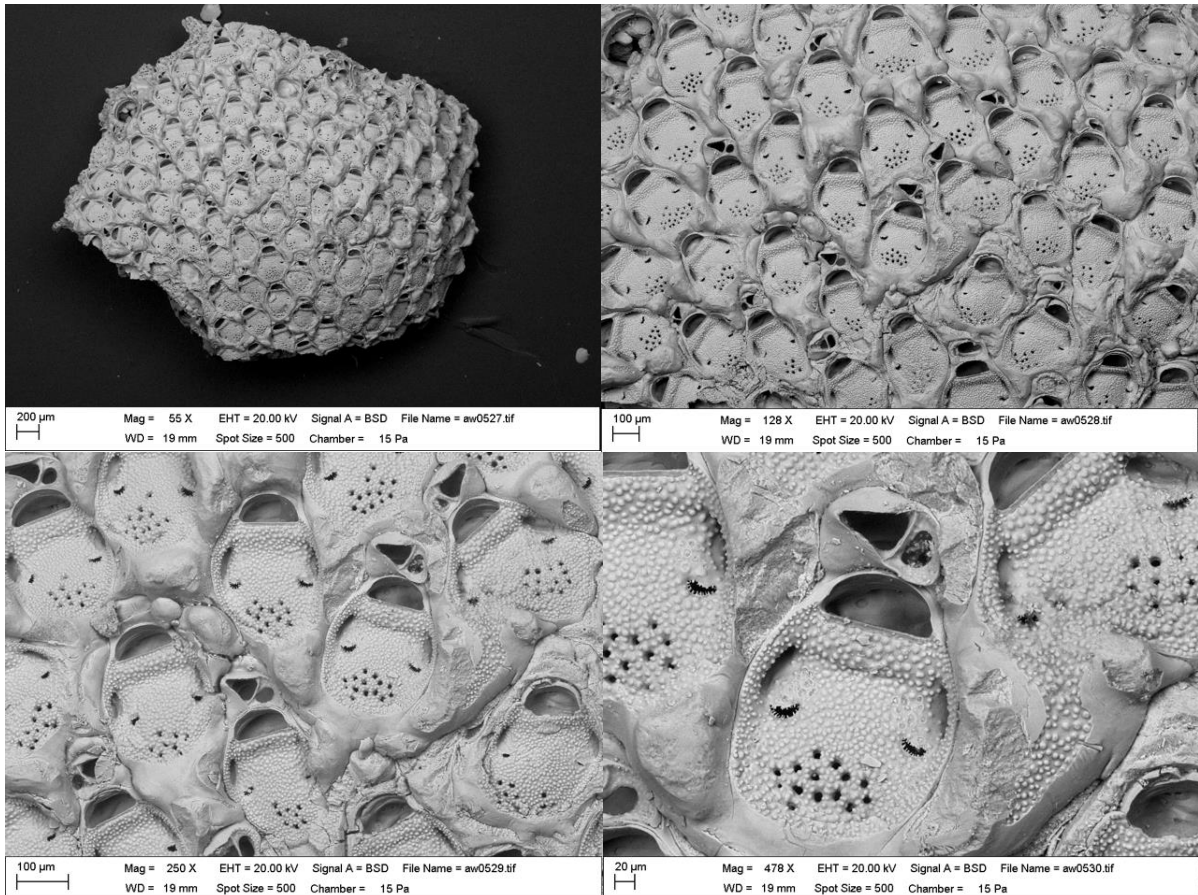Frontal wall: flustrina

Specimen ID: AW730

Pictures credit: Andrea Waeschenbach, NHMUK.

Micropora sp. **Gray, 1848**

Family Microporoidea

Frontal wall: flustraina
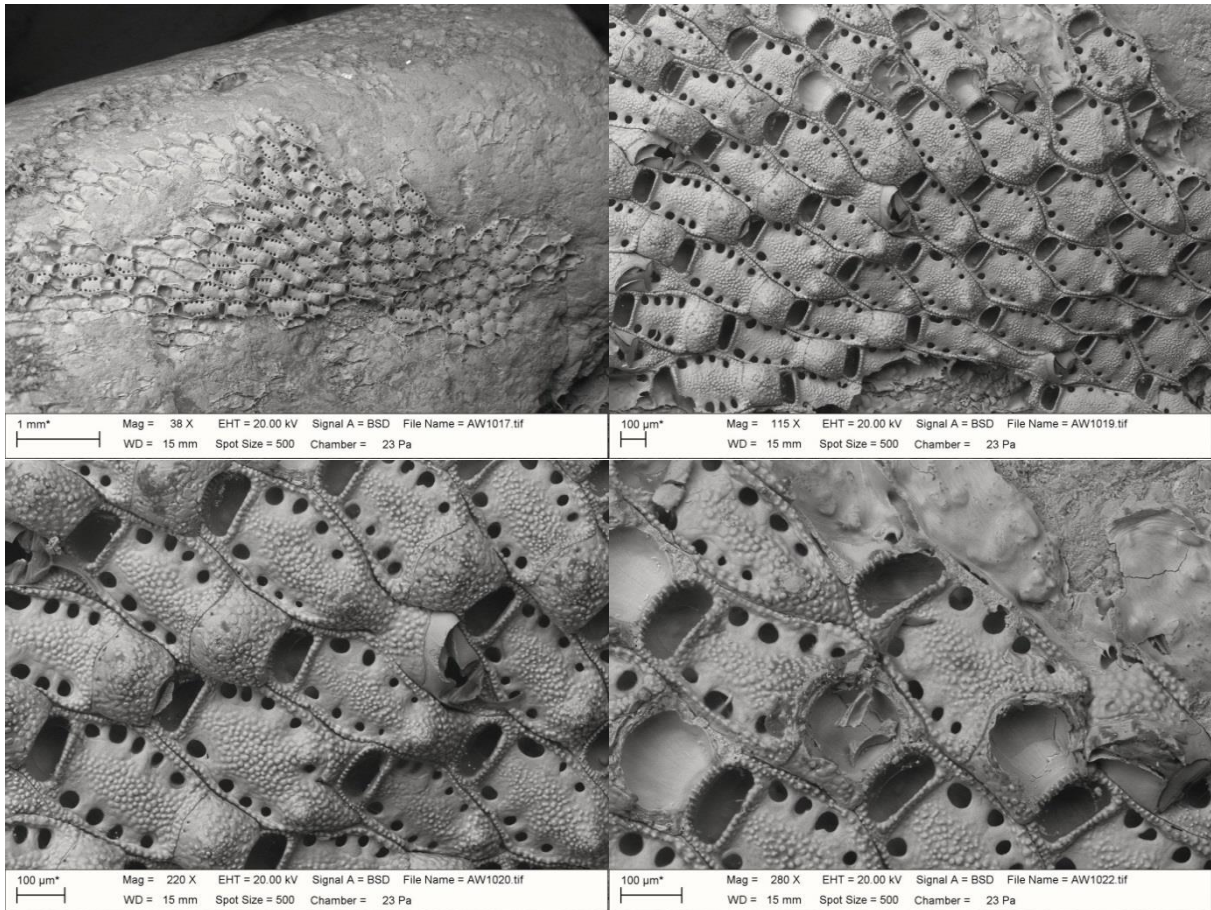
Specimen ID: AW592

Pictures credit: Andrea Waeschenbach, NHMUK.

Opaeophora lepida, **Hincks, 1881**

Family Microporoidea

Frontal wall: flustrina

Specimen ID: AW733

Pictures credit: Andrea Waeschenbach, NHMUK.